CDF/DOC/TRIGGER/CDFR/8415
Version 1.0
September 13, 2006

Proposal for Level-2 Calorimeter Trigger Upgrade

A. Bhatti[1], A. Canepa[2], M. Casarsa[3], M. Convery[1], G. Cortiana[4], M. Dell'Orso[5], G. Flanagan[6], H. Frisch[7], P. Gianetti[5], O. González[8], A. Gresele[4], M. Jones[6], T. Liu[9*], D. Lucchesi[4], M. Piendibene[5], L. Ristori[5], L. Rogondino[5], V. Rusu[7], L. Sartori[5], S. Torre[10], Y. Tu[2], V. Veszpremi[6], M. Vidal[8], S.M. Wang[11]

1 *The Rockefeller University*
2 *University of Pennsylvania*
3 *INFN Trieste*
4 *INFN Padova*
5 *INFN Pisa*
6 *Purdue University*
7 *University of Chicago*
8 *CIEMAT (Madrid)*
9 *Fermi National Accelerator Laboratory*
10 *INFN Frascati*
11 *Academia Sinica*

* Primary contact: thliu@fnal.gov

Abstract

The current CDF Run II Level-2 calorimeter trigger is implemented in hardware and is based on a simple clustering algorithm that was used in Run I. The global transverse energy information is directly passed from Level 1, a strategy that was chosen 25 years ago for a much lower luminosity. This system has worked well for Run II at low luminosity. However, as the Tevatron instantaneous luminosity increases, the limitations due to the simple algorithm have started to become clear. As a result, some of the most important jet and MET related triggers have large growth terms in cross section and already dominate the L2 accept bandwidth at the highest luminosity seen so far ($\sim 180 \times 10^{30}$ cm^{-2}s^{-1}). If not taken care of, they will cause large DAQ deadtime at higher luminosity, and will jeopardize the CDF Run IIb physics program. In this proposal, we will present an upgrade to the L2CAL system which makes the full calorimeter trigger tower information directly available to the L2 decision CPU using Pulsar boards. The upgraded system allows more sophisticated algorithms to be implemented in software; both L2 jets and MET can be made nearly equivalent to offline quality, thus significantly improving the purity as well as the efficiency of the jet and MET related triggers. This is a natural expansion of the already-upgraded L2 trigger system, and is a big step forward to improve the CDF triggering capability at Level 2. We foresee many opportunities for additional improvements in trigger purity and efficiency, most notably for Higgs and exotics triggers, with such information available at Level 2 as dijet mass, $\Delta\phi$ between jets or between a jet and $\not\!\!E_T$, sum E_T of the clusters (H_T), and the possibility of better jet-SVT matching for b-jets.

Executive Summary

Proposal:

- Upgrade L2CAL system by making the full calorimeter trigger tower information directly available to the L2 decision CPU using Pulsar boards, where more sophisticated algorithms can be implemented. This is a natural expansion of the already-upgraded L2 trigger system, and is a big step forward to improve the CDF triggering capability at Level 2 in the face of higher luminosities expected.

Physics motivation:

- Improve the purity of jet and MET related triggers at Level 2.
  This will be required for the survival of important triggers such as the Higgs/SUSY trigger requiring MET and two jets at the highest luminosities.
- Improve the efficiency of triggers requiring multi-jets (top, Higgs) at high luminosity.
- Provide L3-quality calorimeter information at Level 2:
  - Jet E_T, η, ϕ
  - Missing E_T
  - Dijet mass, H_T, $\Delta\phi$ between jets or between jet and $\not\!\!E_T$, b-jet matching with SVT

Cost:

- Using existing Pulsar hardware, the only new hardware which needs to be designed is the mezzanine card. The estimated cost of the mezzanine card is about \$50K, including final production. Details will be discussed at the review on July 27th, 2006.

Schedule:

- We expect the hardware, firmware and software, including system installation, can be done in $\sim$6 months. It may take another few months to fully make use of the new L2CAL trigger capabilities in the official trigger table.

People:

- The project has enough people committed for its successful completion.

Impact on data-taking:

- Commissioning can be done parasitically, as was done for the L2 Pulsar upgrade, minimizing the impact on data-taking.

Level of effort required to extract physics:

- Studies of trigger efficiencies will have to be repeated for existing triggers with calorimeter information provided by the new L2CAL. This will be necessary anyway for the higher luminosity data, even without changes to the current system. Efficiencies are expected to be improved and more stable against luminosity.
- Additional effort by physics groups to improve triggers by taking advantage of the new possibilities allowed by this upgrade could be well worthwhile.

Contents

1 Introduction

The current CDF Run II Level-2 calorimeter trigger is implemented in hardware and is based on a simple algorithm that was used in Run I. This system has worked well for Run II at low luminosity. However, as the Tevatron instantaneous luminosity increases, the limitation due to the simple algorithm starts to become clear. As a result, some of the most important jet and MET related triggers have large growth terms in cross section and already dominate the L2 accept bandwidth at the highest luminosity seen so far ($\sim 180 \times 10^{30}$ cm^{-2}s^{-1}). If not taken care of, they will cause large DAQ deadtime at higher luminosity, and would jeopardize the CDF Run IIb physics program. In this proposal, we will present an upgrade to the L2CAL system which makes the full calorimeter trigger tower information directly available to the L2 decision CPU using Pulsar boards. The upgraded system allows more sophisticated algorithms to be implemented in software; both L2 jets and MET can be made nearly equivalent to offline quality, thus significantly improving the purity as well as the efficiency of the jet and MET related triggers.

This is a natural expansion of the already-upgraded L2 trigger system, and is a big step forward to improve the CDF triggering capability at Level 2. We foresee many opportunities for additional improvements in trigger purity and efficiency, most notably for Higgs and exotics triggers, with such information available at Level 2 as dijet mass, $\Delta\phi$ between jets or between a jet and $\not\!\!E_T$, sum E_T of the clusters (H_T), and the possibility of better jet-SVT matching for b-jets.

This proposal will describe the design, hardware and software implementation, as well as the advantages of this approach over the existing system.

1.1 Overview of the CDF trigger system

CDF Run II trigger is a three level trigger system [1], as shown in Fig. 1. Level 1 (L1) is a synchronous 40 stage pipeline and is based on custom-designed hardware, while Level 2 (L2) is asynchronous and is based on a combination of custom hardware and a commodity processor; Level 3 consists of a processor farm. When an event is accepted by the L1 trigger, all data is moved to one of four DAQ buffers in the front end electronics for all subsystems, and at the same time, subsets of detector information are sent to the L2 system where some limited event reconstruction is performed and a final L2 decision is made. Upon L2 accept, the full detector data is read out and sent to the L3 processor farm for further processing. Only events accepted at Level 3 will be sent to mass storage. The goal of each trigger stage is to reject a sufficient fraction of the events to allow processing at the next stage with minimal dead-time. For the Level-2 trigger, this means that the processing speed should be fast enough (within $\sim$30 microseconds) while the rejection power should be robust enough, which could be challenging at higher luminosity.

To prepare for higher luminosity running of the Tevatron (180×10^{30} cm^{-2}s^{-1} has already been achieved, while in the near future the peak is expected to be as high as 300×10^{30} cm^{-2}s^{-1}), many subsystems in the CDF trigger system have already been upgraded in the

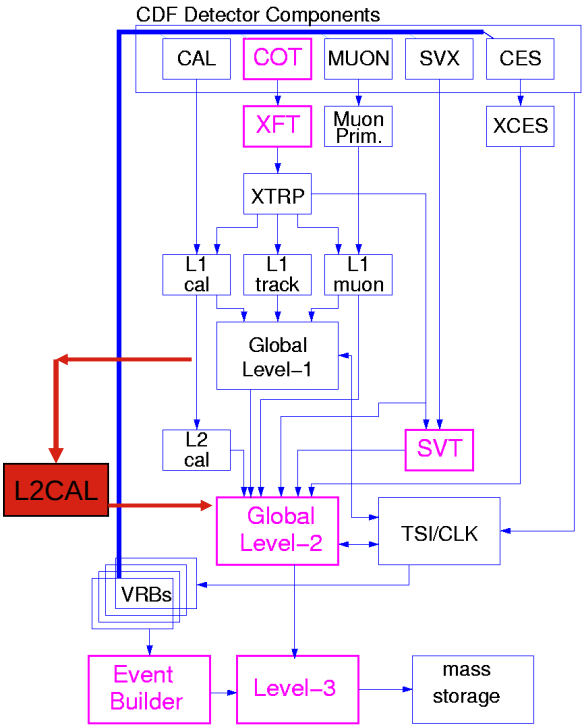

Figure 1: Overview of the CDF trigger. The red box represents the proposed L2CAL upgrade.

past few years (shown in pink in Fig. 1). The L1 Track Trigger (XFT) is being upgraded to improve its trigger purity. The L2 SVT and Global decision subsystems have been upgraded to improve the processing speed. Both the Event Builder and L3 processor farm have been upgraded to increase the bandwidth downstream of Level 2. In February 2006, at record luminosity 180×10^{30} cm^{-2}s^{-1}, we learned that the system is limited by the L2Accept bandwidth. Due to the improvements made to the event builder and L3 processing farm during the shutdown, we expect the L2 accept limit to be improved, however, not beyond $\sim$1 kHz. Note also that the maximum available L2 bandwidth decreases as the instantaneous luminosity increases due to higher occupancies.

At $\mathcal{L}$ $\sim$180$\times$10^{30} cm^{-2}s^{-1}, the L2 accept rate is already beyond $\sim$800 Hz with many L2 trigger cross sections growing rapidly with instantaneous luminosity. In order to survive, we need to improve the L2 rejection power at higher luminosity. The triggers with large growth terms fall into three main categories: 1) triggers involving CMX; 2) triggers involving jets and MET; and 3) backup triggers. For example, both the high-p_T CMX trigger and the trigger requiring MET plus two jets are already each running at $\sim$100 Hz at Level 2 at $\mathcal{L}$ $\sim$180E30. The cross section for the MET+2JET trigger as a function of luminosity is shown in Fig. 2. Backup triggers (which are essential as control samples for important high-p_T physics) by their very nature have high growth terms. Although they do not dominate the L2 accept bandwidth at current luminosities, they will at the highest luminosities. This

makes it even more important to improve the rejection power (i.e. purity) for the triggers in categories (1) and (2). We expect the ongoing XFT upgrade, once finished, will make the triggers in category (1) manageable. This leaves category (2) to be dealt with.

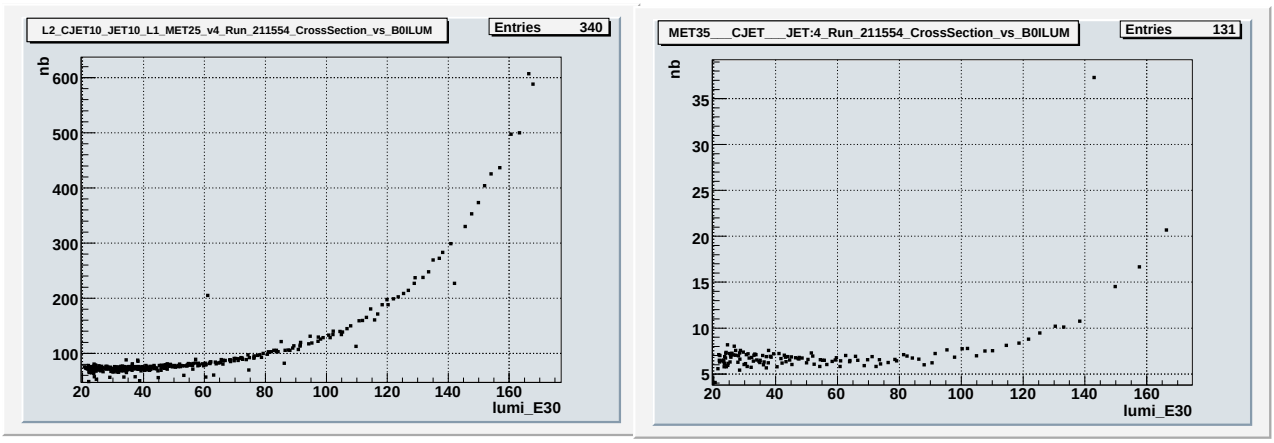

Figure 2: Cross section vs. luminosity for the Higgs/SUSY trigger requiring MET and two jets (*left*) at Level 2 (L2_CJET10_JET10_L1_MET25_v4) and (*right*) at Level 3 (MET35_&_CJET_&_JET).

In this proposal, we will describe an upgrade for the L2CAL subsystem (shown in red in Fig. 1, requiring only modest effort) to significantly improve its trigger rejection power at higher luminosity and at the same time, improve its capability and flexibility in order to increase its trigger efficiency for important high p_T physics processes.

1.2 The existing CDF calorimeter trigger

The goal of the calorimeter trigger (both at Level 1 and Level 2) is to trigger on electrons, photons, jets, total event transverse energy (SumET), and missing transverse energy (MET). For CDF Run II, all calorimeter tower energy information, including both Electromagnetic (EM) energy and Hadronic (HAD) energy, is digitized every 132 ns and the physical towers are summed into trigger towers, weighted to yield transverse energy. A trigger tower covers 15° in azimuth ϕ and approximately 0.2 in pseudo-rapidity η [2]. This results in a representation of the entire detector as a 24×24 map in the η-ϕ plane. The trigger tower energy data is then sent to both the L1 and L2 calorimeter trigger systems with 10-bit energy resolution, using a least significant count of 125 MeV, and resulting in a full scale E_T of 128 GeV. At Level 1, L1CAL only uses 8-bit trigger tower energy information for L1 processing, with the two least significant bits dropped. As examples, electron and photon triggers are formed at L1CAL by simply applying energy thresholds to the EM energy of a trigger tower, and jet triggers are formed using the total EM+HAD energy of a trigger tower. For electrons, tracks from the L1 track trigger (XFT) can be matched to the trigger towers while HAD energy can be used for rejection. L1CAL also calculates the event SumET and MET using the lower resolution 8-bit EM+HAD energy information.

At Level-2, the L2CAL subsystem receives all 10-bit trigger tower energy information. However, the existing hardware-based L2CAL system does not re-calculate the event SumET and MET using the full resolution energy information available; rather, it still uses the SumET and MET information directly from L1CAL. This design feature limits its trigger selection capability, or rejection power, for triggers with global transverse energy requirements. A good example is the MET plus two jet trigger shown previously. The main task of the existing L2CAL is to find clusters using the E_T of the trigger towers. The cluster-finding algorithm is based on a simple algorithm used for Run I ("Pac-man"), and is implemented in hardware. In this simple algorithm, the L2CAL hardware forms clusters by simply combining contiguous regions of trigger towers with non-trivial energy. Each cluster starts with a tower above a "seed" threshold (3 GeV) and all towers above a second lower "shoulder" threshold (1 GeV) that form a contiguous region with the seed tower are added to the cluster. The size of each cluster expands until no more shoulder towers adjacent to the cluster are found. The cluster location is simply taken to be the location of the seed tower, which is biased towards lower η and ϕ. Since the seed tower is just the first tower found above the seed threshold, its location could be far from the true jet centroid, especially at high luminosity when the calorimeter occupancy is high. The existing L2CAL trigger system has worked reasonably well at lower luminosity for Run II, however, as the occupancy in the calorimeter increases with luminosity, the simple hardware-based L2CAL system starts to lose its rejection power. In particular, the higher occupancy (largely due to multiple interactions per beam crossing) in the calorimeter has already been observed in the past to produce large fake clusters with high (fake) E_T in the L2CAL system, resulting in a high L2 accept rate saturating the bandwidth downstream of L2 at high luminosity. The jet triggers L2_JET40, JET60, and JET90 are examples; the cross sections for JET40 and JET60 are shown in Fig. 3.

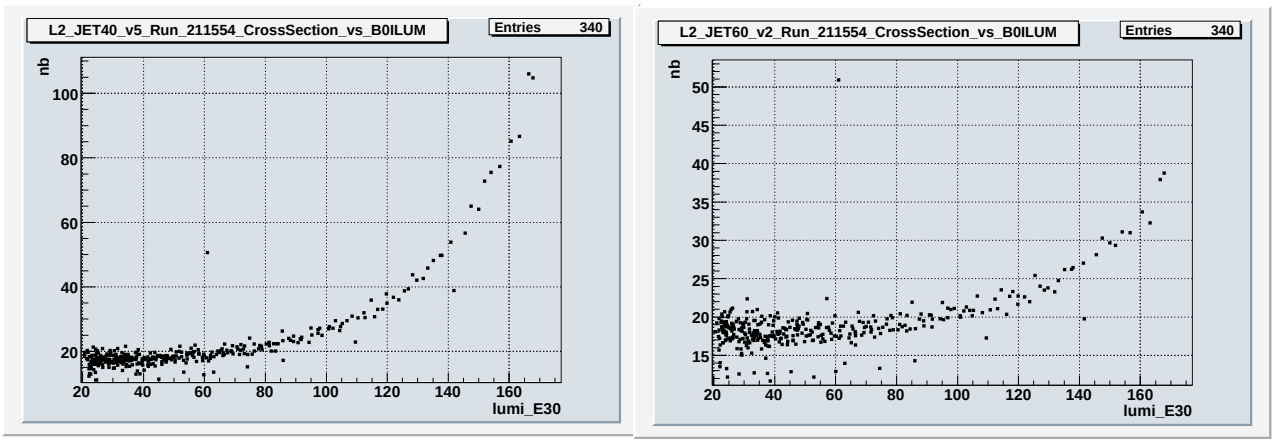

Figure 3: Cross section vs. luminosity for the L2_JET40 and L2_JET60 triggers.

1.3 L2 calorimeter trigger upgrade

In this proposal, we will describe an upgrade path for the L2CAL system. This upgrade approach is based on the Pulsar board [3], a general purpose VME board developed at CDF and used for upgrading both the L2 global decision crate [4] and the L2 silicon vertex tracking (SVT) subsystem [5]. In this approach, the full resolution calorimeter trigger tower data would be received, preprocessed and merged by a set of Pulsar boards before being sent to the Level-2 decision CPU running a cluster-finding algorithm. The challenges of this upgrade, which we will show can be mastered, are to keep the clustering algorithm processing latency within ∼20 microseconds, and to have minimal impact of the running experiment during commissioning. Since the actual cluster-finding is done inside the CPU, it is much more flexible. The clustering algorithm is more robust against increasing luminosity (higher occupancy in the calorimeter system). For example, the large fake clusters with large fake E_T will be eliminated since the CPU algorithm will not blindly combine contiguous regions of trigger towers. In addition, the event SumET and MET can be re-calculated using the full resolution 10-bit trigger tower energy information available to L2. The proposed L2CAL upgrade allows more sophisticated algorithms to be implemented.

Jet reconstruction using a cone algorithm which is currently being done at Level 3 can be moved to Level 2, albeit clustering trigger towers (instead of physical towers) and using only a single iteration in order to save processing time. We will show that L2 jets found using the proposed algorithm are nearly equivalent to offline jets in terms of E_T, centroid, and efficiency, a vast improvement over the current situation. The calculation of MET at Level 2 with resolution closer to that at Level 3 will reduce L2 rates for Higgs and SUSY triggers that require $\not\!\!E_T$, which will be vital for preserving these triggers at high instantaneous luminosity.

Although the main goal of the upgrade is to significantly reduce the growth terms of the existing jet and MET related triggers, the proposed L2CAL upgrade for CDF will make the full-resolution trigger tower information directly available to the L2 decision CPU. This is a big step forward in improving the CDF triggering capability at Level 2. There are two aspects: to have enough flexibility to deal with potential new challenges at the highest luminosities, and to improve CDF new physics search sensitivities beyond the baseline. For example, the new system would allow the possibility to trigger on dijet mass, $\Delta\phi$ between dijets or between a jet and $\not\!\!E_T$, sum E_T of the clusters (H_T), and better jet-SVT matching for b-jets. In addition, together with the XFT upgrade which makes ∼3D tracking information available at Level 2, this might provide a means to improve important tau triggers at Level 2.

The next section will describe in more detail the features and limitations of the current L2 calorimeter trigger system. The remainder of the proposal will describe the design, hardware and software implementation, commissioning strategy, as well as the advantages of this approach over the existing system.

2 The current Level-2 jet and MET triggers

2.1 Limitations of the current L2 jet clustering

As previously described, the current CDF Level-2 hardware-based jet clustering trigger uses the same algorithm as was used in Run I. Its simple "Pac-man" algorithm, described in Sec. 1.2, breaks at high instantaneous luminosities. As the underlying event energy increases with the number of interactions (beam backgrounds could also contribute), calorimeter towers which are unrelated to any jet activity have their E_T boosted above clustering thresholds. Towers above shoulder threshold between true jets can link multiple jets together into a single cluster. Clusters of a huge number of low-E_T towers can be formed which do not include a true jet at all. Figure 4 shows a "phase-transition" between true jets containing fewer, higher-E_T towers, and fake clusters which combine a large number of tower together which push the cluster above threshold. Figure 5 shows an example of a cluster passing the L2_JET90 trigger which is made up of 70 towers, some of which belong to true low-E_T jets. The "Pac-man" nature of the algorithm is clearly seen. These fake clusters are the source of the rapid growth in cross section with luminosity (Fig. 3).

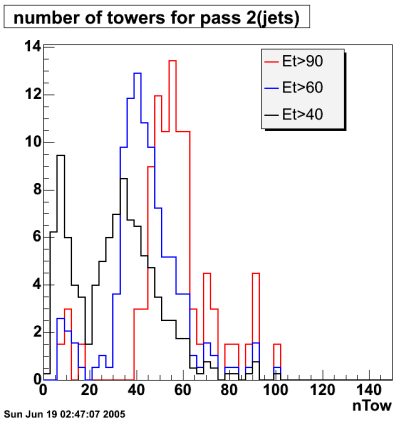

Figure 4: Histogram of the number of towers in L2_JET40, 60, and 90 clusters in a run taken at $\mathcal{L} \sim 90$-120×10^{30} cm^{-2}s^{-1} (taken prior to removal of the Ring-of-Fire from the trigger, discussed later).

The tendency of the "Pac-man" algorithm to group jets into a single cluster also reduces the efficiency for triggers requiring multiple jets at Level 2. Figure 6 shows an event display from an event with large $\not\!\!E_T$ and two offline jets which failed the MET+2JET trigger because the two jets were merged by the L2 clustering. Also shown in Fig. 6 is the efficiency for the MET+2JET trigger as a function of offline $\not\!\!E_T$, measured using high-p_T muon data requiring $E_T^{jet1} > 35$ GeV and $E_T^{jet2} > 24$ GeV. Studies have shown that the drop in efficiency at high $\not\!\!E_T$ is due to merging of jets at Level 2. For offline jets which are well separated, the measured trigger efficiency is higher. Besides this important Higgs trigger, top and other triggers requiring multiple jets could suffer from this loss of efficiency at high luminosity (studies are in progress).

Another property of the "Pac-man" clusters is that even when the cluster is associated with a true jet, the cluster E_T, and also η and ϕ (taken simply from the location of the seed tower) are on average a poor match to the true jet properties.

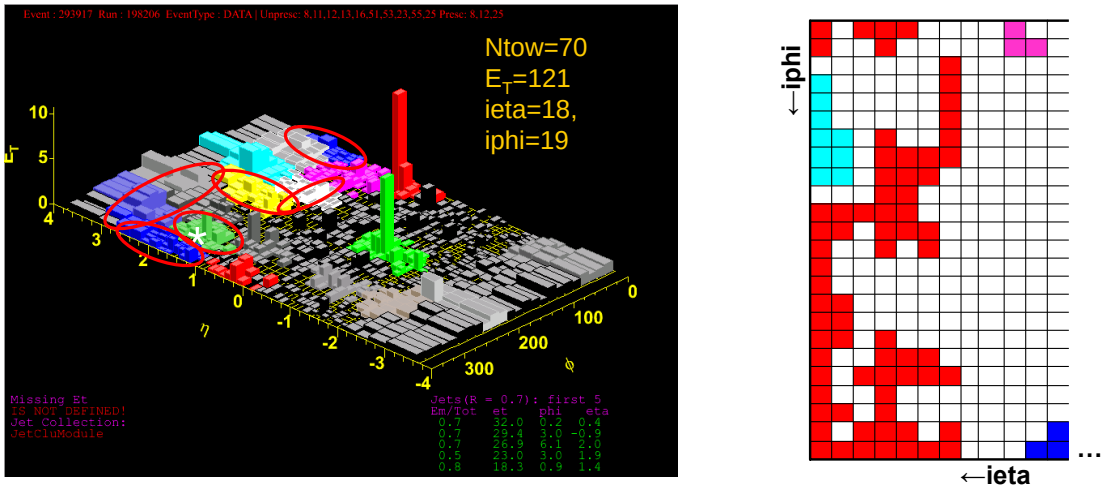

Figure 5: (*left*) An example of a large cluster (70 towers) which passes the L2_JET90 trigger but is rejected by JET100 at Level 3. (*right*) The towers represented by red squares are clustered together as a single jet.

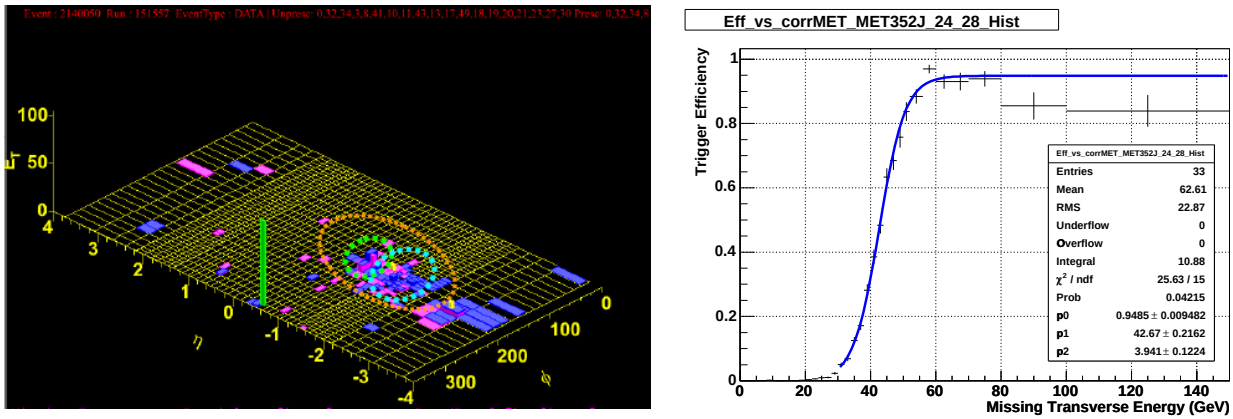

Figure 6: (*left*) A two-jet event with large MET, seen as a single jet at Level 2. (*right*) Efficiency of the trigger requiring MET and two jets as a function of (offline) MET, measured using high-p_T muon data requiring $E_T^{jet1} > 35$ GeV and $E_T^{jet2} > 24$ GeV. This trigger is used for $ZH \to \nu\nu bb$ as well as SUSY searches. The drop in efficiency at high MET is due to merging of jets at the trigger level.

2.2 Attempts to improve L2 clustering using the current hardware

In early 2005, it became clear that the L2_JET trigger cross sections had a large growth term due to high activity in the highest-$|\eta|$ trigger towers known as the "Ring-of-Fire" (ROF). In fact, Fig. 5 is a perfect example of a ROF-induced fake cluster. In summer 2005, towers in the ROF were dis-allowed as shoulder (or seed) towers for a L2 cluster. The growth with luminosity dropped dramatically (Fig. 7) up to the highest luminosities seen at the time, $\mathcal{L} \sim 100 \times 10^{30}$ cm^{-2}s^{-1}. However, later on, a growth term re-emerged at higher luminosities. Studies made during the design of the Run IIb trigger table focused on keeping the highest-E_T jet trigger (JET100) unprescaled. Increasing the threshold at Level 1 from 10 to 20 GeV was found to reduce the JET100 cross section with minimal impact on efficiency. Figure 8 shows that this reduced the cross section for current luminosities, but that a growth term is again re-emerging at higher luminosities. Also, the lower-E_T L2_JET triggers were left unimproved and destined to be given heavy prescales (see Fig. 3).

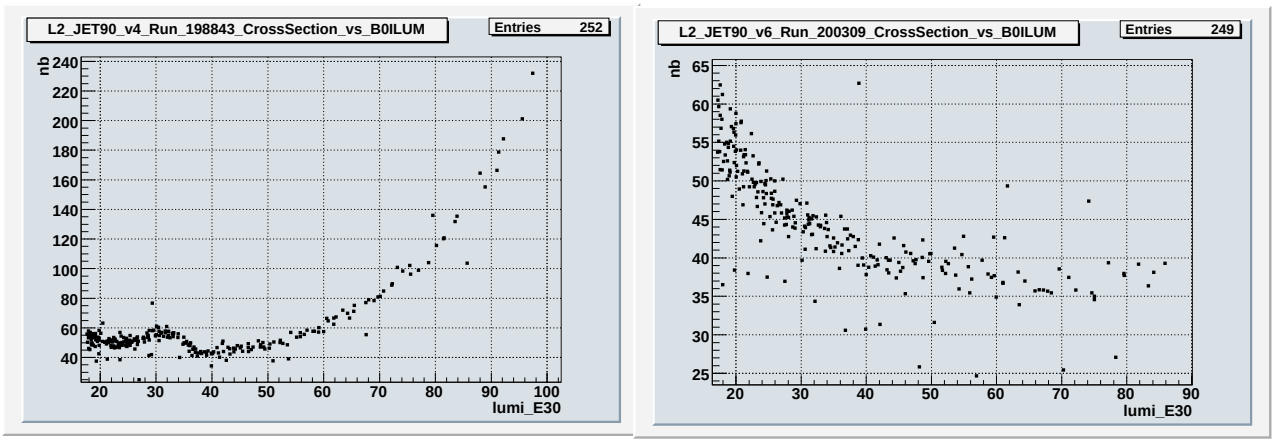

Figure 7: L2_JET90 cross section (*left*) before and (*right*) after the highest-η trigger towers (Ring-of-Fire) were removed from the trigger.

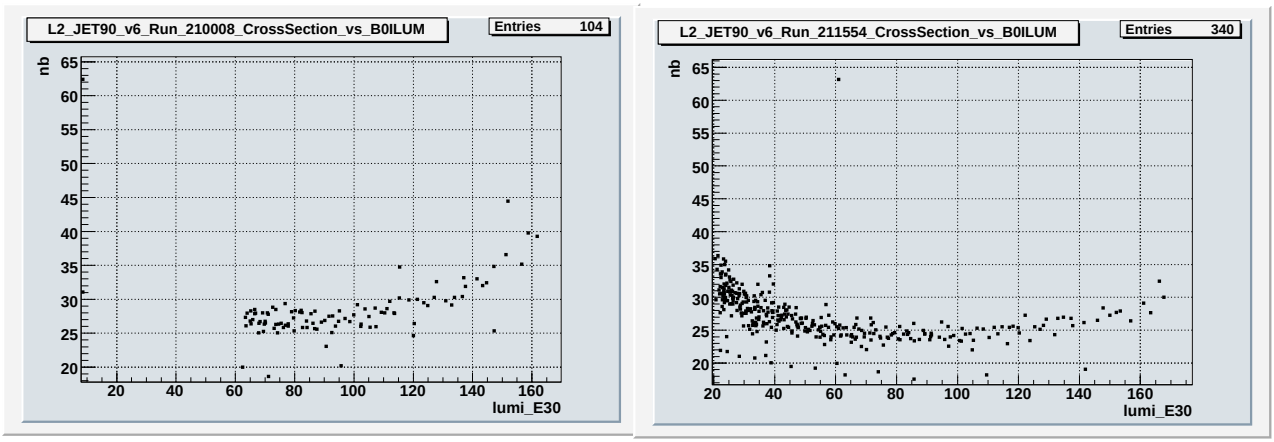

Figure 8: L2_JET90 cross section (*left*) before and (*right*) after the L1 requirement was changed from a single trigger tower of 10 GeV to the new requirement of 20 GeV.

In a final attempt to save these triggers using the existing L2 clustering hardware, studies were conducted where shoulder thresholds were raised in order to break up runaway "Pac-man" clusters. Figure 9 shows for L2_JET40 that increasing the shoulder threshold from 1 GeV to 1.5 GeV appears to remove the growth of the number of fake clusters with luminosity, up to luminosities of $\sim 160 \times 10^{30}$ cm^{-2}s^{-1}. However, Fig. 10 shows that this leads to too great a loss of efficiency for triggering on low-E_T jets. Note that many important triggers require low-E_T jets at Level 2.

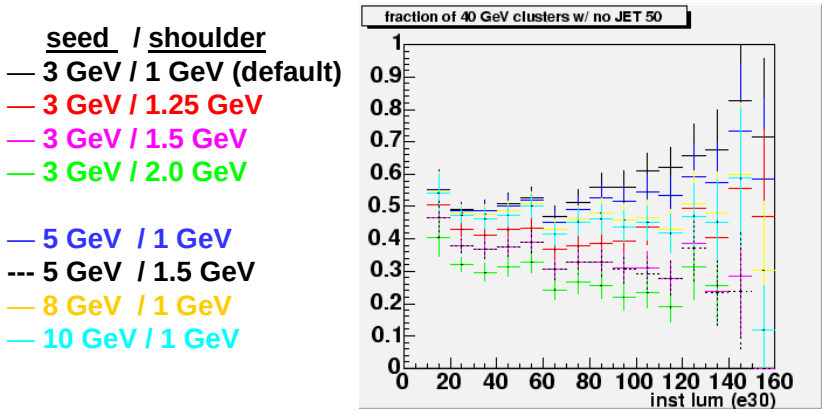

Figure 9: Fraction of 40 GeV L2 clusters which do not pass the L3 JET50 trigger as a function of different clustering thresholds and instantaneous luminosity. Note that valid jets with $40 < E_T < 50$ GeV fall into this category, as well as fake clusters.

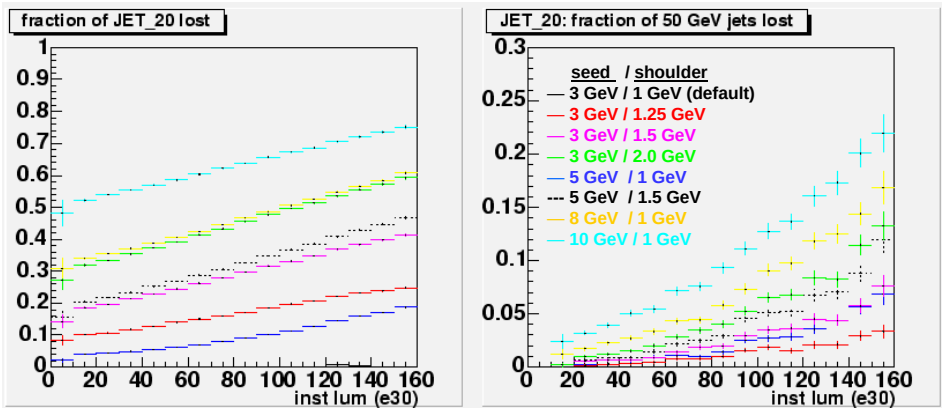

Figure 10: Fraction of events lost in the JET20 sample as a function of luminosity and different clustering thresholds. Note that although the L1 trigger requires a 5 GeV tower, raising the seed threshold to 5 GeV can still cause events to be lost if the 5 GeV tower is not part of the > 20 GeV jet.

2.3 The current MET triggers

So far we have described the L2 jet triggers. The $\not\!\!E_T$ at Level 2 is simply taken from the L1 MET which uses 8-bit trigger tower information. The MET triggers are also characterized by cross sections which grow rapidly with instantaneous luminosity. The cross section for the current inclusive $\not\!\!E_T$ trigger (L2_MET35) is shown in Fig. 11.

The Higgs/SUSY trigger requiring MET and two jets (MET+2JET) has an enormous growth term as well (see Fig. 2). The rate cannot be controlled by cutting harder either on the MET or the jet threshold. In fact the cut on MET is already too hard and is cutting deep into the signal acceptance as shown in Fig. 12 for the Higgs in the $ZH \to \nu\nu bb$ channel. (We have already shown the loss of efficiency for this trigger due to the merging of jets at high luminosity and that we cannot raise the shoulder threshold for such low-E_T jets.) In the current situation, there is no hope for maintaining the efficiency of this trigger for Higgs searches while controlling the cross section at the highest instantaneous luminosities. With attention focused on the light Higgs, this would be embarrassing for CDF.

As detailed in the following sections, the L2CAL upgrade will provide the full calorimeter 10-bit trigger tower information to the L2 decision CPU. This will directly improve the MET and jet-E_T resolution at Level 2. In addition, other calorimeter information such as the $\Delta\phi$ between the $\not\!\!E_T$ and jets could be made available and used to improve the trigger purity (and therefore cross section), if needed. Figure 13 shows the improvement in the trigger turn-on that could be gained with just the increased precision in the MET calculation. The reduction of the growth term of the MET triggers from the proposed calculation of $\not\!\!E_T$ at Level 2 will be shown in Sec. 3.1.6.

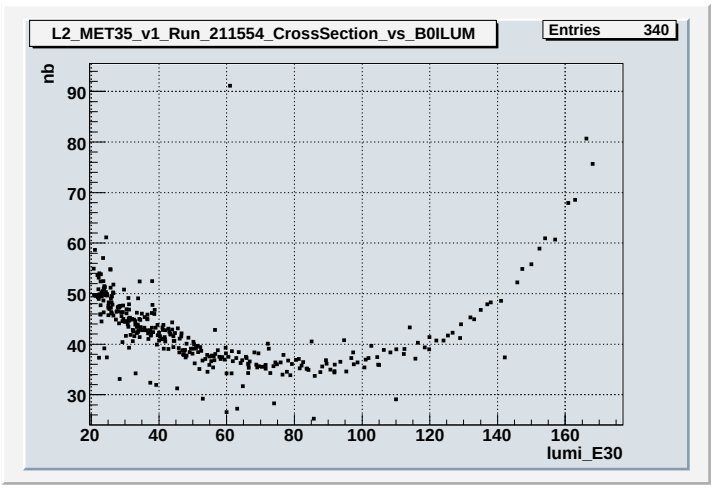

Figure 11: Cross section as a function of instantaneous luminosity for the L2 trigger requiring $\not\!\!E_T > 35$ GeV.

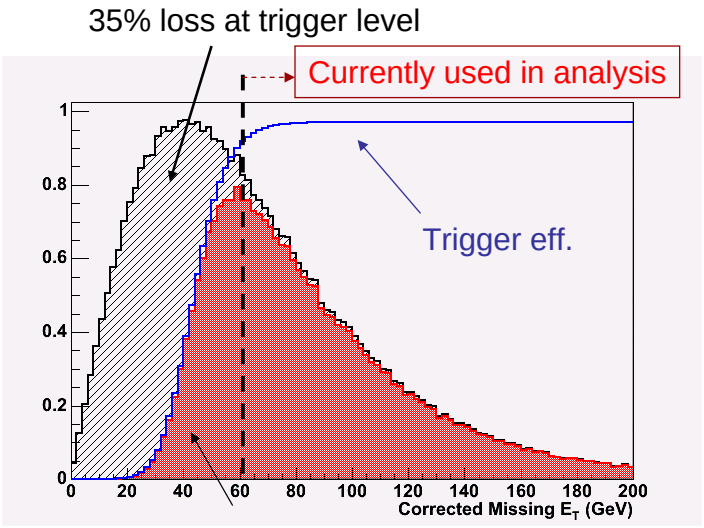

Figure 12: Expected signal shape as a function of corrected $\not\!\!E_T$ of the SM Higgs assuming $M_H = 120$ GeV for the Higgs search in the $ZH \to \nu\nu bb$ channel. The blue curve shows the efficiency of the trigger requiring MET and two jets currently used, and the red histogram shows the signal acceptance due to the trigger. Approximately 50% of the signal is lost after applying a an offline cut to avoid systematic uncertainties in the trigger turn-on.

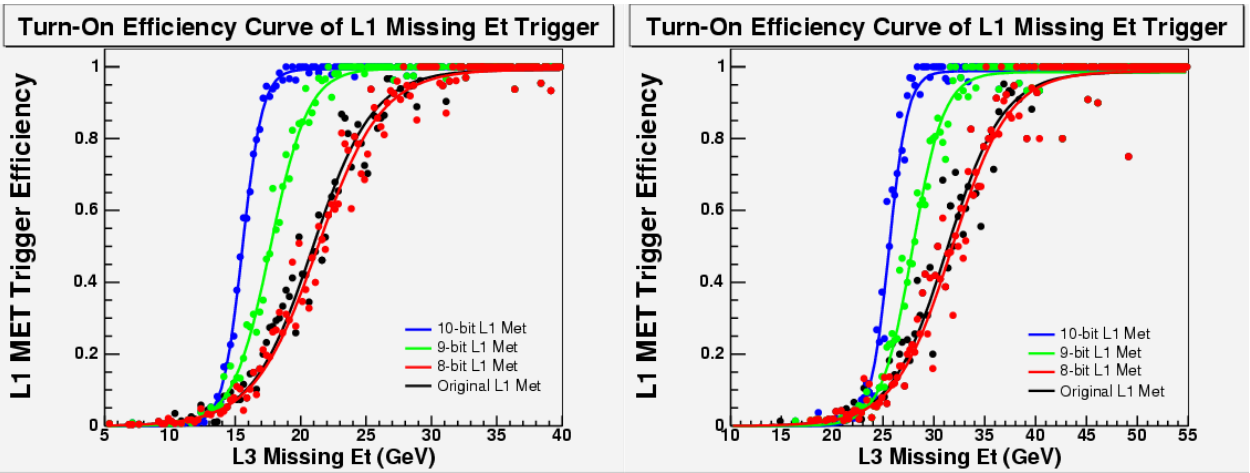

Figure 13: L1 MET trigger efficiency of (*left*) $\not\!\!E_T > 15$ GeV and (*right*) $\not\!\!E_T > 25$ GeV cuts for 8 (current), 9, and 10 bit precision of the MET calculation. L1_MET25 is currently used in the MET+2JET and inclusive MET triggers. The proposed upgrade will provide 10-bit precision at Level 2.

3 Proposed upgrade to Level-2 jet and MET triggers

In this proposal, we will present an upgrade to the L2CAL system which makes the full calorimeter trigger tower information directly available to the L2 decision CPU using Pulsar boards. The upgraded system allows more sophisticated algorithms to be implemented in software; both L2 jets and MET can be made nearly equivalent to offline quality, thus significantly improving the purity as well as the efficiency of the jet and MET related triggers. The hardware upgrade will be described in Sec. 4. Although this provides a wealth of information which can be used to improve trigger performance, we describe in this section only improvements in the basic trigger objects: jets and MET. (Other studies, for example on $t\bar{t}$ MC, are in progress.)

The jet triggers are improved by using a cone algorithm in the L2 CPU for jet cluster finding. The proposed L2Cone algorithm is outlined below. It is similar to JetClu (which is used to reconstruct L3 and offline jets) except that the clustering is done in a single iteration, in order to save processing time.

1. Order trigger towers above seed threshold in E_T.
2. Beginning with the highest-E_T seed, sum the E_T of all towers that satisfy a shoulder threshold in a cone of $R = 0.7$ around the seed. Also calculate the E_T-weighted η and ϕ of the cone.
3. Flag those towers as used.
4. Repeat (2) and (3) using the next unused seed tower until all seeds are used.
5. Return a list of the first 20 "L2Cones" sorted in decreasing E_T (having more than 20 doesn not make a difference).

The following sections will show that the L2Cone jets are much better matched to offline jets in E_T, η, and ϕ than the current L2Clusters; in fact they are nearly of offline quality. The growth of the cross section with luminosity which was due to the runaway "Pac-man" clusters is greatly reduced.

The MET will be recalculated in the L2 CPU using the full resolution 10-bit trigger tower energy information, instead of using the L1 MET calculated with 8-bit precision, as is currently done. The improved $\not\!\!E_T$ resolution, again of almost offline quality, reduces the growth with luminosity of the cross section for the inclusive MET trigger and has an even stronger effect on the growth term of the MET+2JET trigger.

3.1 Performance study

In this section we compare the performance of the jet and MET triggers in the existing and proposed systems. For the jet triggers, the Ring-of-Fire has been excluded from the L2Clusters online, but not from the L2Cones. Ideally, the ROF towers should also be removed from the offline jet reconstruction for a proper comparison with L2Clusters, however, the

information needed to do this is not readily available in the data ntuple since it requires rerunning the offline clustering. For the studies presented here, we look first at events where the leading offline jets do not include towers in the ROF. Note that we expect the performance of the L2Cone algorithm to be fairly independent of η, while the L2Cluster algorithm is expected to perform better in the central region than in the higher-occupancy plug. We first want to understand the basic performance in the region where both algorithms are expected to perform well. In Sec. 3.1.2, we will first show plots where the ROF has been avoided by restricting the offline jets to have their centroid within the central region $|\eta| < 1.0$. Next we include the plug, but still exclude any offline jets which contain towers in the ROF ($|\eta| > 2.6$), which essentially results in the jet centroid being within $|\eta| <\sim 2$ (see Fig. 14). The final comparisons in Sec. 3.1.4 will show the differences in performance at all η between the L2Clusters which do not include towers in the ROF and the L2Cones which have no restrictions on the ROF. This will include the effects of excluding the ROF in the current L2Clusters. For those comparisons, we will not make a restriction on the η of offline jets, and will ask whether a given offline jet was found (within a given $\eta - \phi$ distance of the offline jet) by L2Cluster and/or L2Cone, and how well the E_T of the L2 jet matches that of the offline jet.

We show results for the existing L2Cluster algorithm, the proposed L2Cone with the same seed and shoulder thresholds (3 GeV and 1 GeV, respectively), L2Cone in the ideal case with seed and shoulder thresholds of 0, as well as L2Cone with various intermediate thresholds which allow the algorithm to run reasonably fast on the L2 CPU. The final choice of thresholds will have to balance between algorithm speed and the physics trigger improvements.

Improvements in the growth rate of the trigger cross sections with luminosity are studied using an unbiased data sample which requires a single trigger tower above threshold at Level 1. In addition to the improvements to jet trigger rates due to the proposed clustering algorithm, we have also investigated the improvements to MET trigger rates gained by replacing the current L2 MET, simply taken from L1, with the proposed L2 MET calculation. This single-tower sample can be used for both jets and MET because the L2 jet triggers require a single-tower trigger at Level 1, and the L2 MET triggers should not be biased by a low-threshold single-tower requirement. It also has the advantage that the single-tower trigger cross section is relatively independent of instantaneous luminosity.

We have used a subset of the gjs0ai (JET_CAL_SINGLETOWER_5, hereafter referred to as STT5) and gjs1bi (JET_CAL_SINGLETOWER_10, STT10) datasets taken at instantaneous luminosities $\mathcal{L}$ ∼100-170×10^{30} $\mathrm{cm}^{-2}\mathrm{s}^{-1}$ to compare the L2 clustering algorithm and offline jets (JetClu with cone size 0.7).

Figs. 15-21 give an overview of the STT5 sample used in the studies: the instantaneous luminosity, the offline leading-jet E_T, η, and ϕ, and the L2Cone E_T, η, and ϕ for L2Cones found using seed and shoulder thresholds of 0 and a maximum of 20 L2Cones returned.

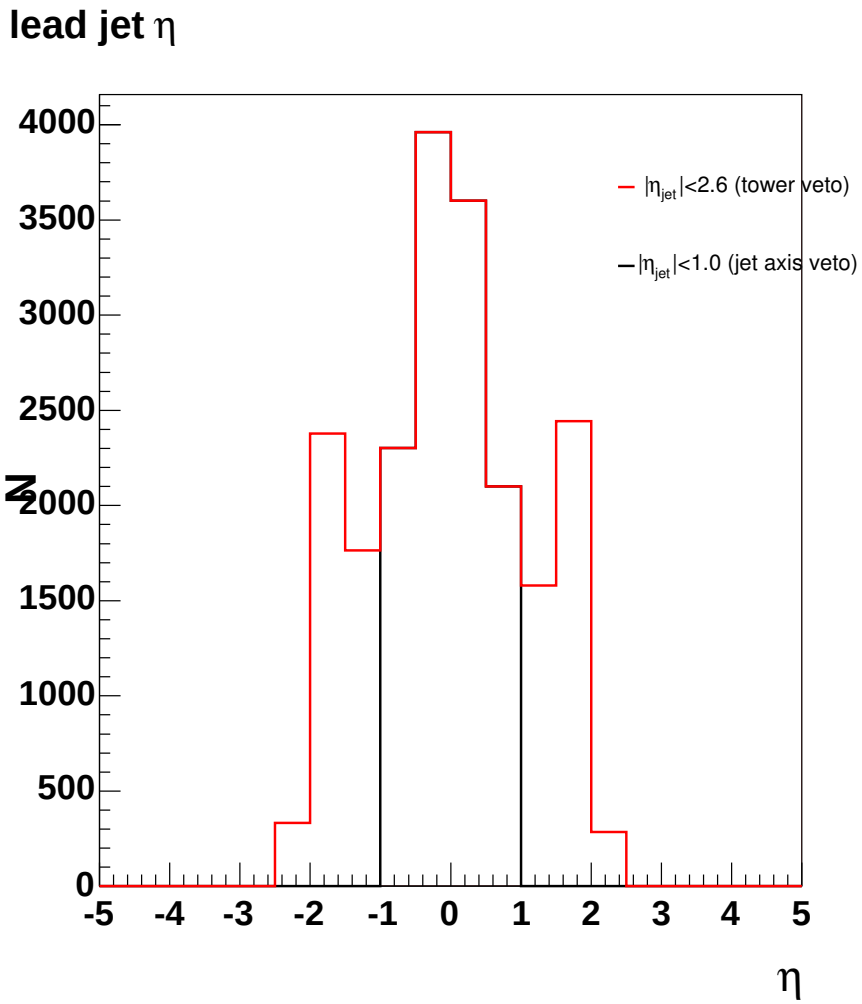

Figure 14: Centroid η of offline leading jets for the requirements made in order to avoid the ROF.

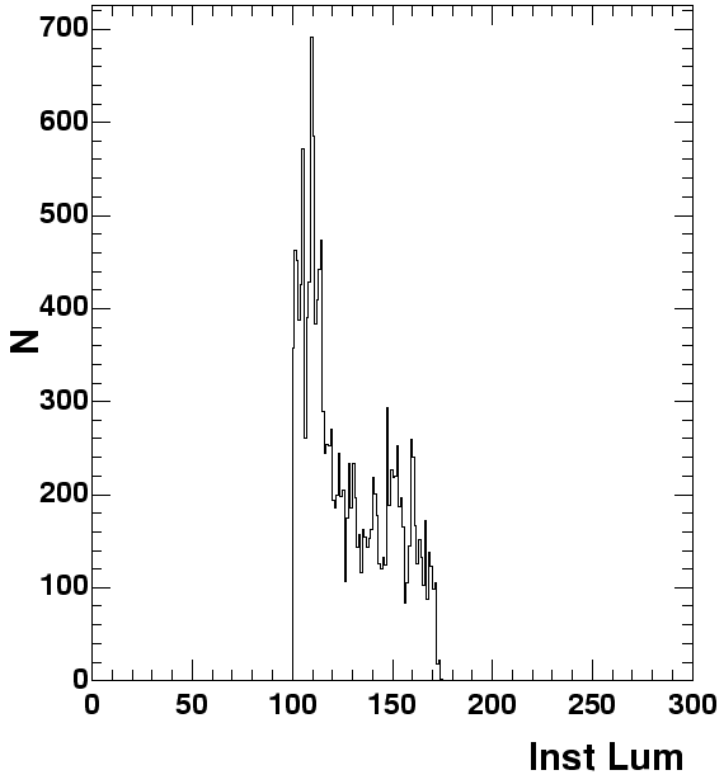

Figure 15: Instantaneous luminosity of the test sample (gjs0ai data).

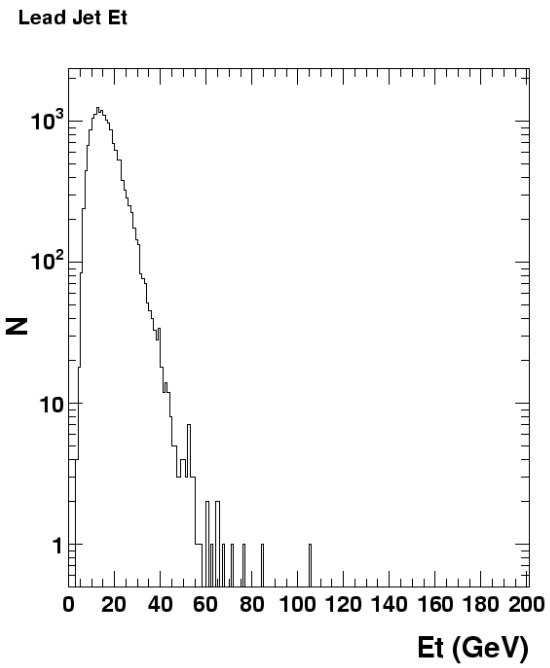

Figure 16: Offline leading jet E_T in the test sample.

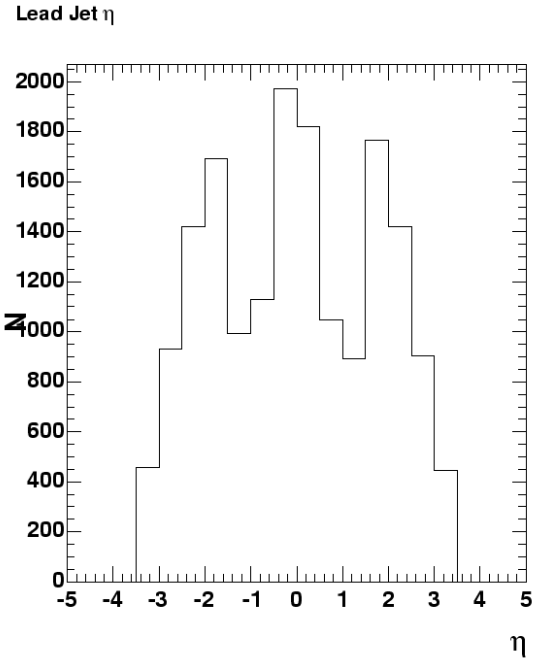

Figure 17: Offline leading jet η in the test sample.

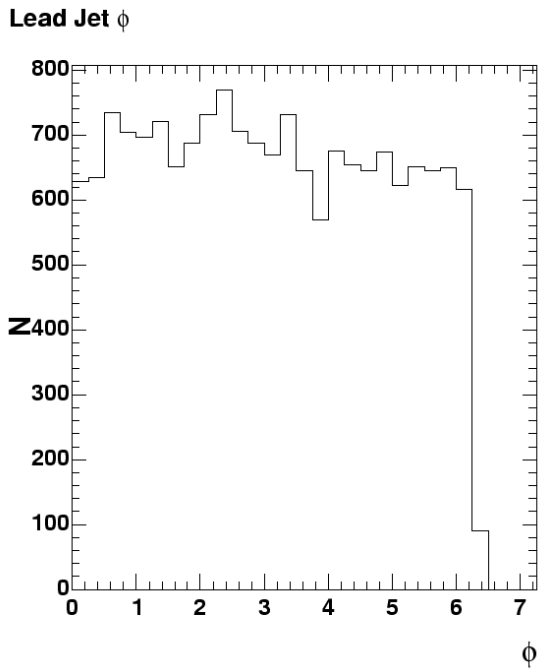

Figure 18: Offline leading jet ϕ in the test sample.

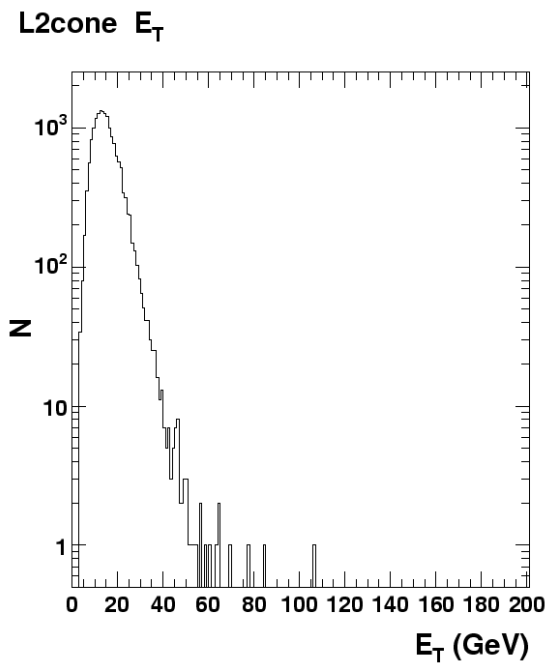

Figure 19: L2Cone E_T in the test sample (seed, shoulder threshold of 0).

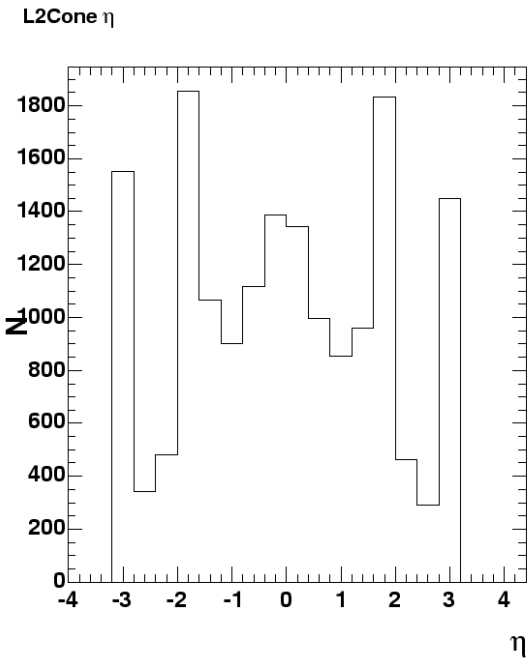

Figure 20: L2Cone η in the test sample (seed, shoulder threshold of 0).

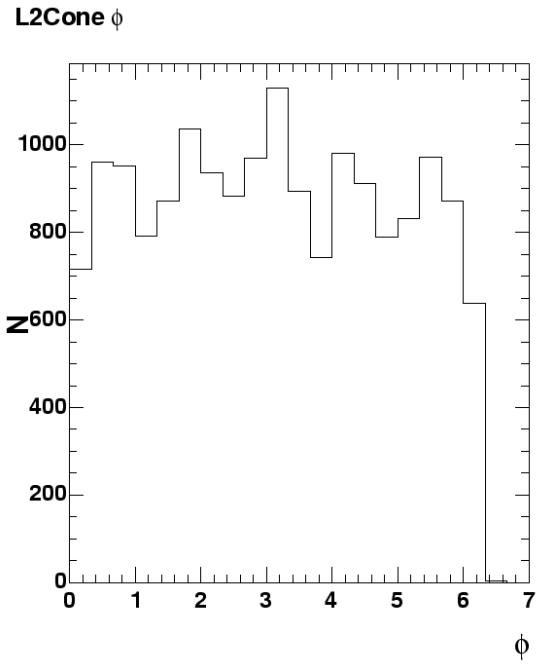

Figure 21: L2Cone ϕ in the test sample (seed, shoulder threshold of 0).

3.1.1 Matching L2 jets to offline jets

In order to examine the performance of the L2 clustering, we need to compare L2 jets to offline jets. The leading offline jet is used, and is matched to the nearest L2 jet. We match the L2 jets to offline jets in (η, ϕ) by finding the pair with the smallest distance between them, $min[\Delta R = \sqrt{(\Delta\phi)^2 + (\Delta\eta)^2)}]$. Figure 22 shows the ΔR distribution between offline and current L2Cluster or proposed L2Cone jets.

The leading offline jet may not contain a trigger tower which would pass the seed threshold, in which case the nearest L2 cluster found may correspond to a different offline jet; this is what causes the entries at large ΔR which are not seen when the offline jet is required to contain a 5 GeV trigger (Fig. 22). Therefore, a 5 GeV L1 seed for the offline jet was required for all of the following plots in this section, except where specifically noted. Figure 23 shows a zoomed in view of the ΔR distribution including also the result for L2Cones with seed and shoulder thresholds of zero.

3.1.2 Comparison of basic L2 clustering performance away from the Ring Of Fire

Figures 24-29 show results of the proposed L2Cone algorithm using a seed threshold of 3 GeV and a shoulder threshold of 1 GeV, compared to results from the current L2Cluster (which uses those thresholds). The offline jets are required to have a 5 GeV L1 seed. Figures 24 and 25 show that the η and ϕ of the L2Cones are well matched to the offline jet position. The E_T resolution is shown in Fig. 26. Figure 27 shows the average L2 jet E_T vs. the offline jet E_T. The correlation for L2Cones is quite good, while the L2Clusters are poorly matched in E_T with the offline jets. Because of the 5 GeV seed tower requirement, low-E_T jets in this sample tend to consist of a single tower, thus giving the false sense that the L2Cluster algorithm performs well at low-E_T. For this reason, we also look at a minimum-bias data sample with no 5 GeV seed tower requirement, shown in Fig. 28. There we see that the L2Cluster algorithm is inefficient at low E_T as well.

Returning to the STT5 sample, the E_T distribution is shown for limited bands of offline jet E_T Figs. 29-36 for a shoulder threshold of 1 GeV for both L2Cluster and L2Cone, and for a shoulder threshold of 0.5 GeV for L2Cone. Again, better agreement is seen between the L2Cone and offline jet E_T than for L2Cluster.

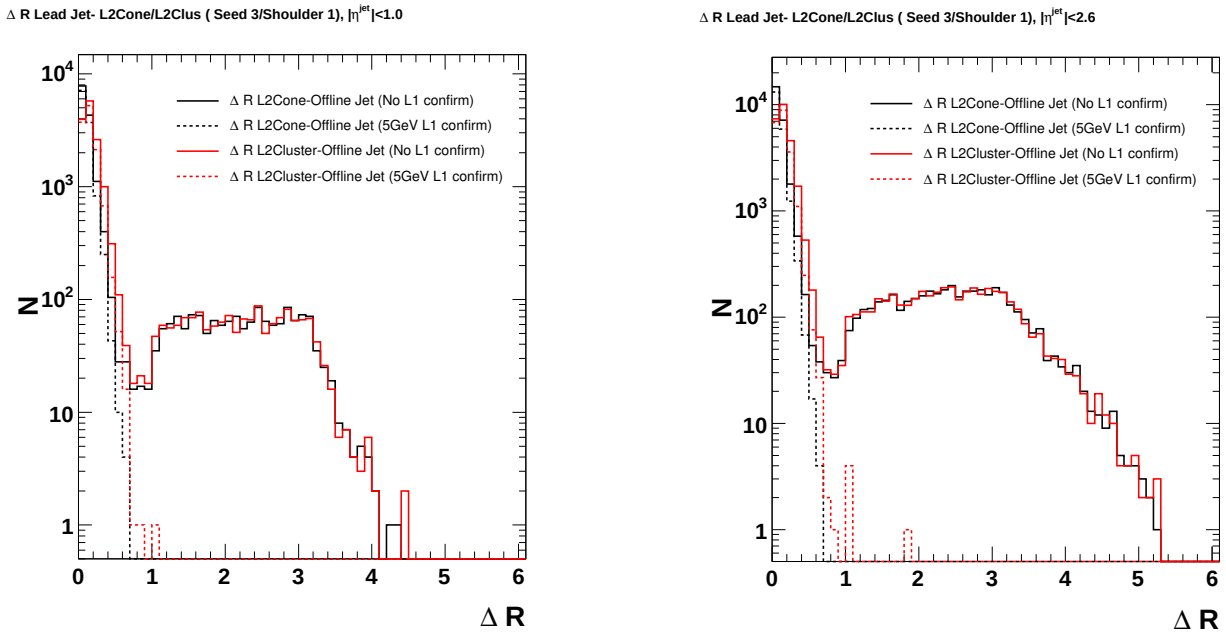

Figure 22: ΔR between leading jet and the matched L2Cone (*black*) or the matched L2Cluster (*red*). The dashed curves show the effect of requiring the leading jet to have a 5 GeV L1 seed. (*left*) offline jets restricted to $|\eta| < 1.0$. (*right*) offline jets restricted to have no towers in the ROF ($|\eta| > 2.6$).

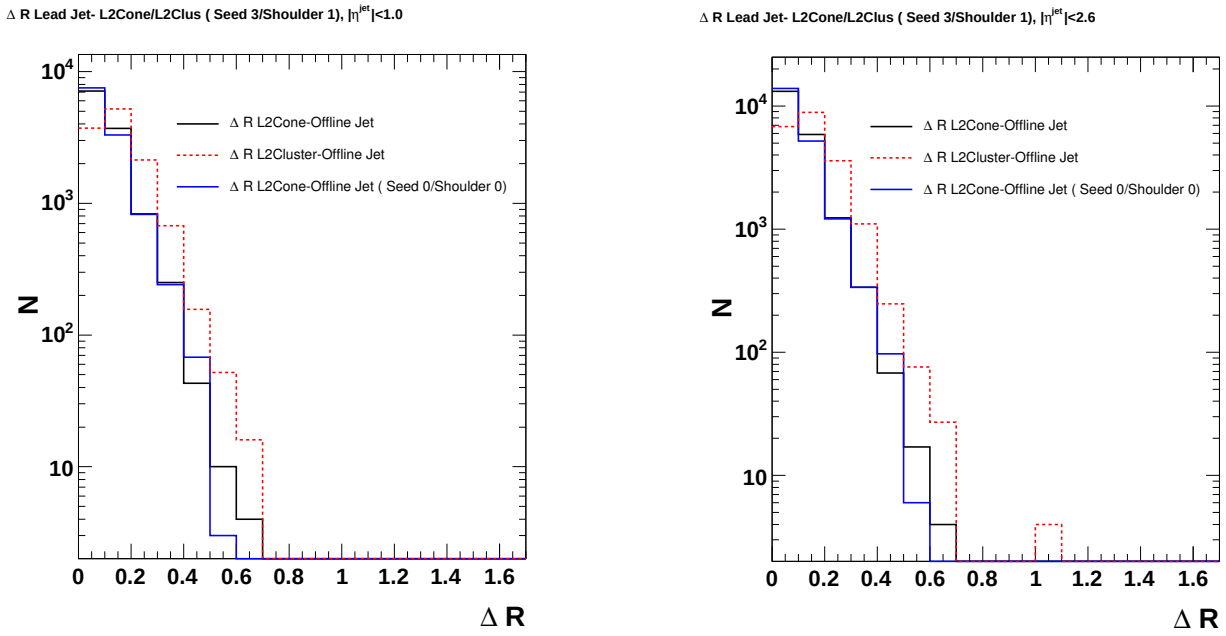

Figure 23: ΔR between leading jet and the matched L2Cone (*black*) or the matched L2 cluster (*red*) with seed (shoulder) threshold of 3 (1) GeV. The matched L2Cone in the ideal case with thresholds 0 (0) GeV is also shown (*blue*). (*left*) offline jets restricted to $|\eta| < 1.0$. (*right*) offline jets restricted to have no towers in the ROF ($|\eta| > 2.6$).

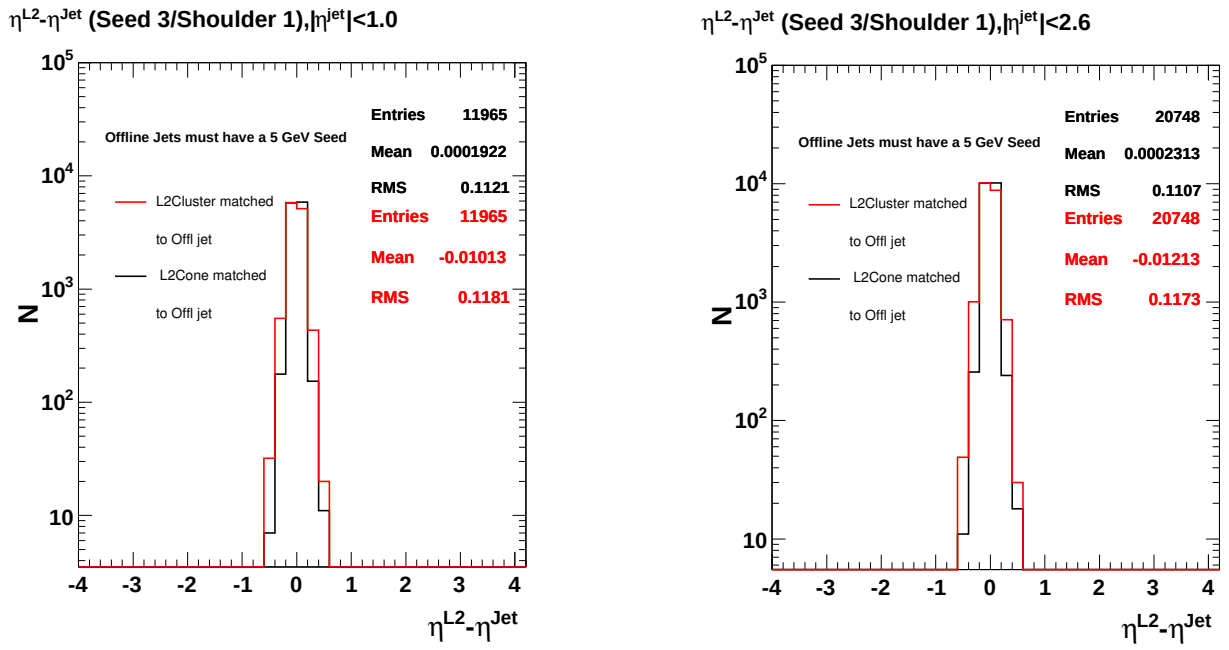

Figure 24: $\Delta\eta$ between leading jet and the matched L2Cone (*black*) or the matched L2Cluster (*red*). (*left*) offline jets restricted to $|\eta| < 1.0$. (*right*) offline jets required to have no towers in the ROF ($|\eta| > 2.6$).

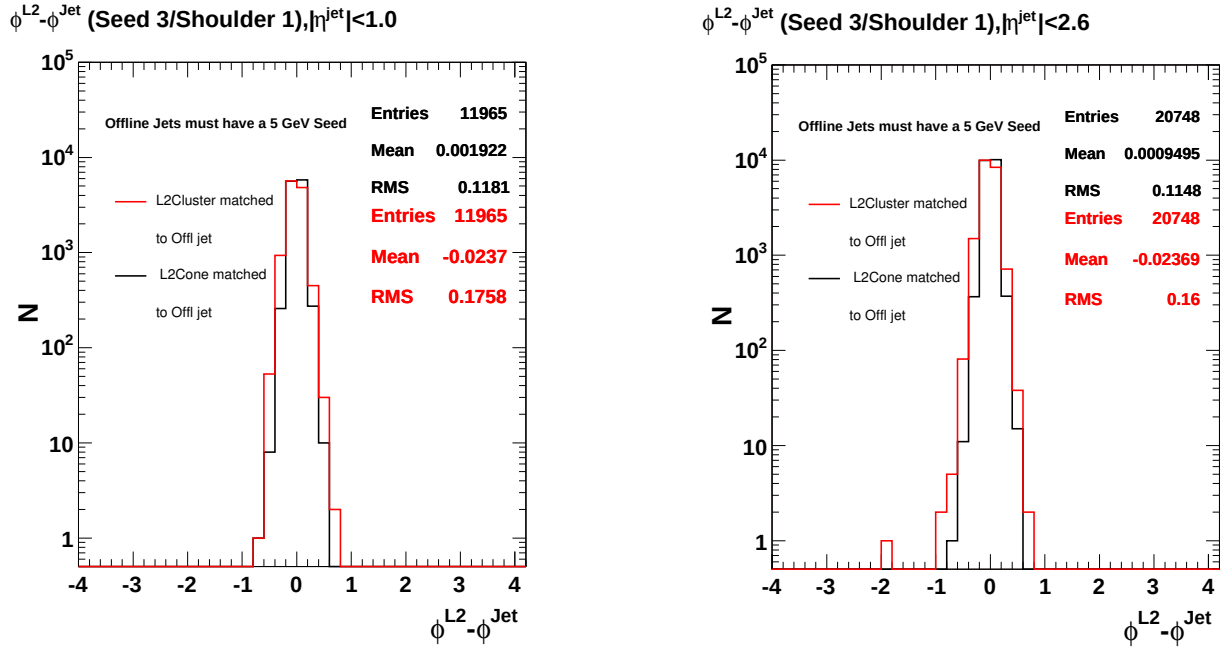

Figure 25: $\Delta\phi$ between leading jet and the matched L2Cone (*black*) or the matched L2Cluster (*red*). (*left*) offline jets restricted to $|\eta| < 1.0$. (*right*) offline jets required to have no towers in the ROF ($|\eta| > 2.6$).

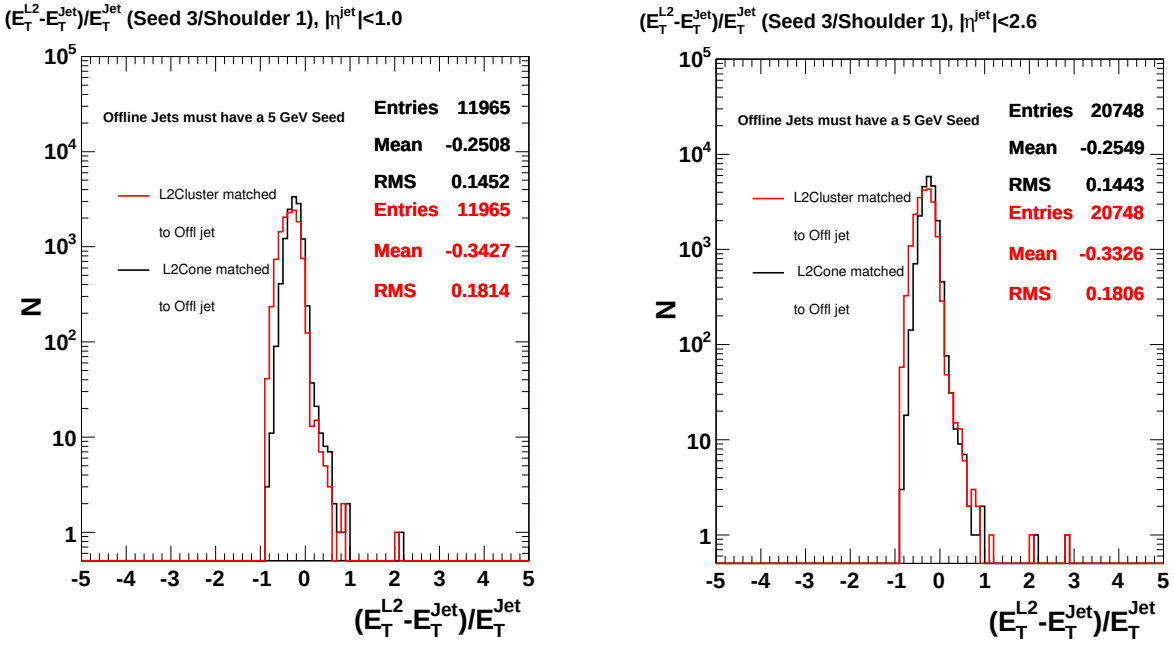

Figure 26: $(E_T^{L2} - E_T^{jet})/E_T^{jet}$ between leading jet and the matched L2Cone (*black*) or the matched L2Cluster (*red*). (*left*) offline jets restricted to $|\eta| < 1.0$. (*right*) offline jets required to have no towers in the ROF ($|\eta| > 2.6$).

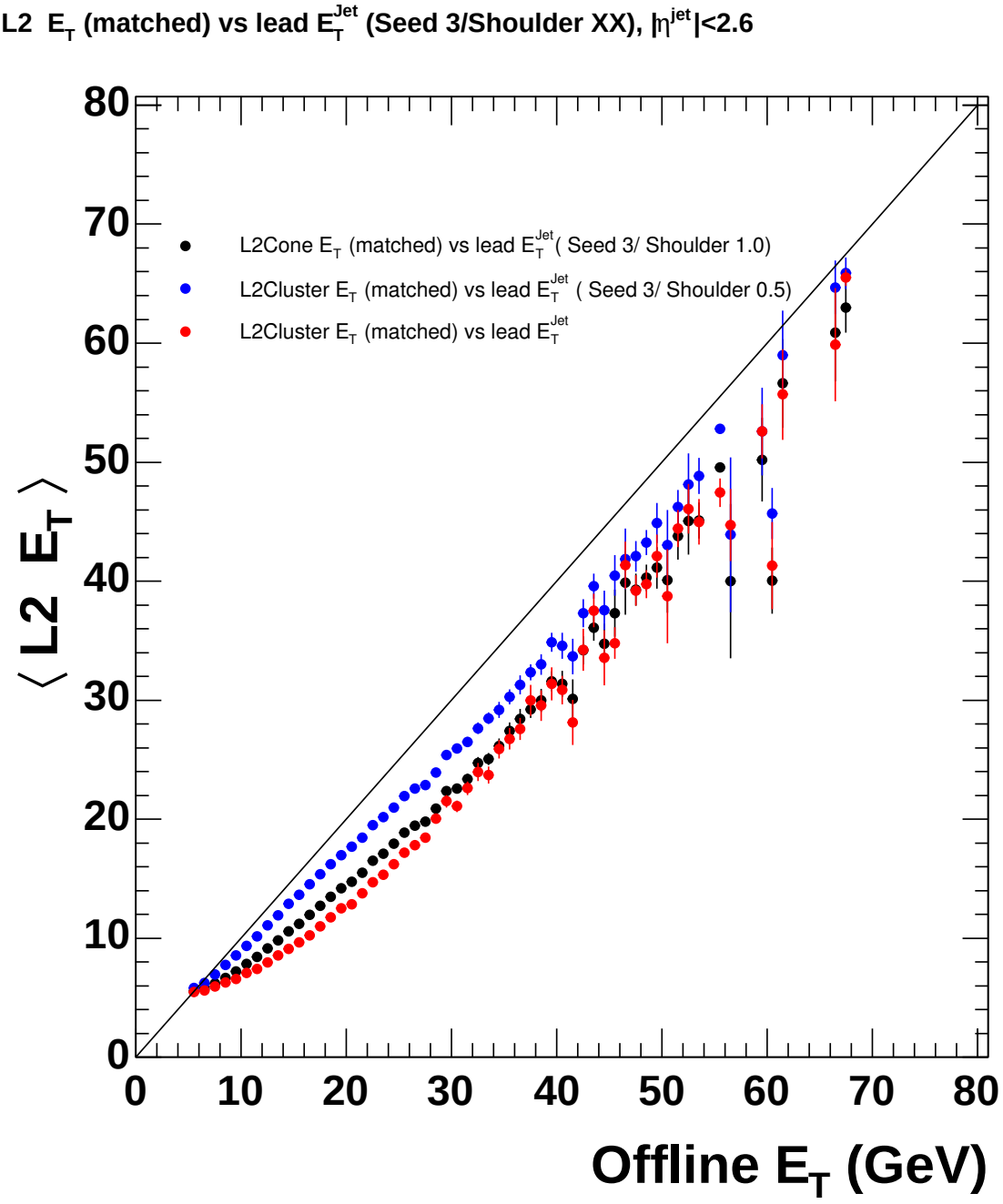

Figure 27: Correlation of average E_T between L2Cone (*black*), L2Cone with shoulder threshold 0.5GeV, or L2Cluster (*red*), and leading offline jet E_T. Offline jets are restricted to have no towers in the ROF region $|\eta| > 2.6$. The leading jet is required to have a 5 GeV L1 seed.

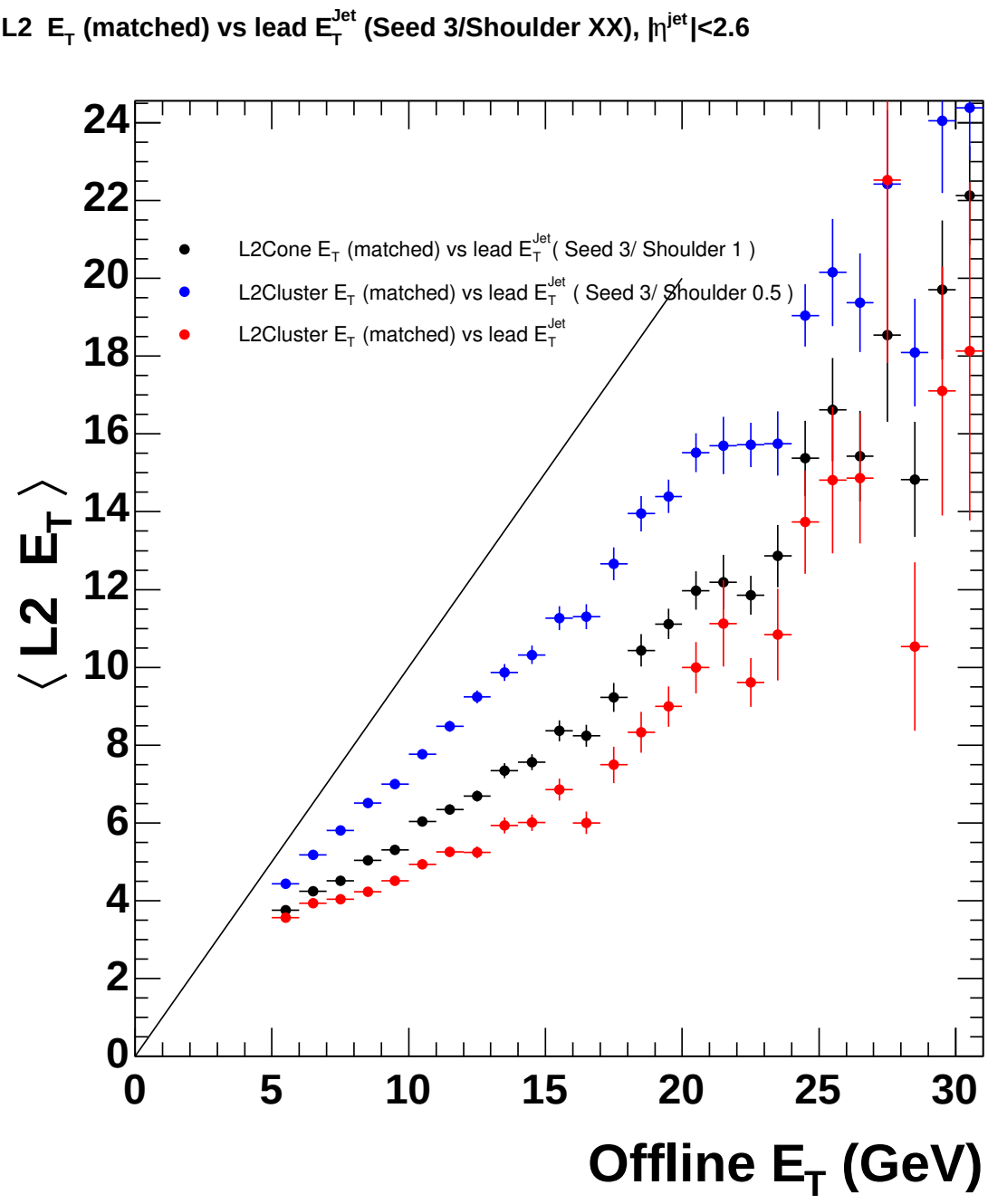

Figure 28: Correlation of average E_T between L2Cone (*black*), L2Cone with shoulder threshold 0.5GeV, or L2Cluster (*red*), and leading offline jet E_T, using a min-bias sample without the 5 GeV seed requirement in order to see the performance for low-E_T jets.

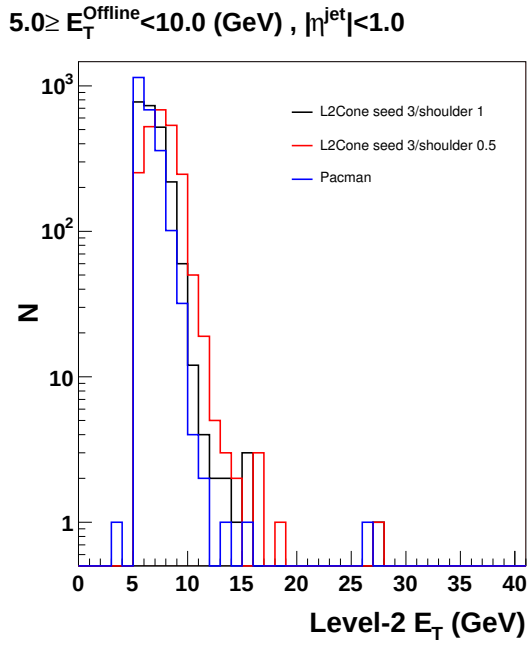

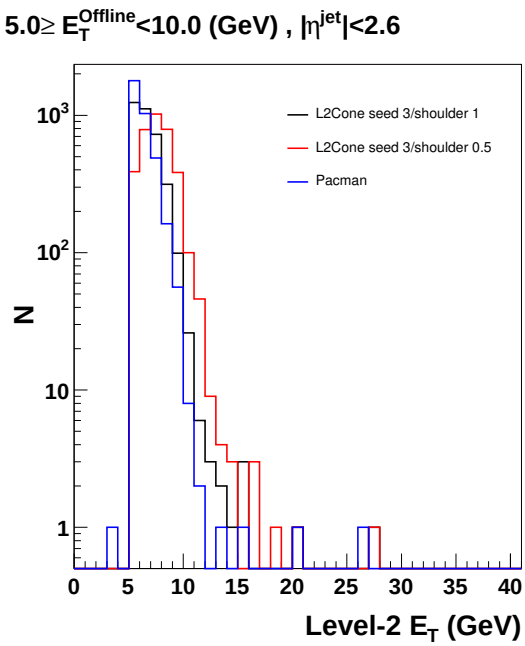

Figure 29: E_T distribution of L2Cones (*black*) and L2Clusters (*red*) corresponding to offline jets with E_T in the range $5 < E_T < 10$ GeV. (*left*) offline jets restricted to $|\eta| < 1.0$. (*right*) offline jets restricted to have no towers in the ROF $|\eta| > 2.6$.

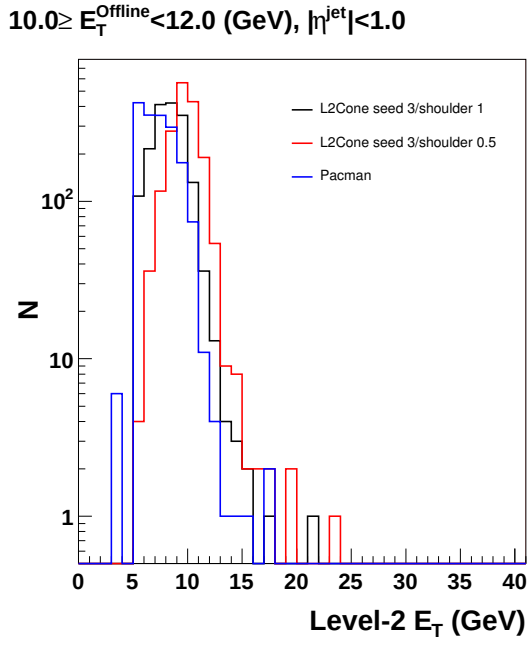

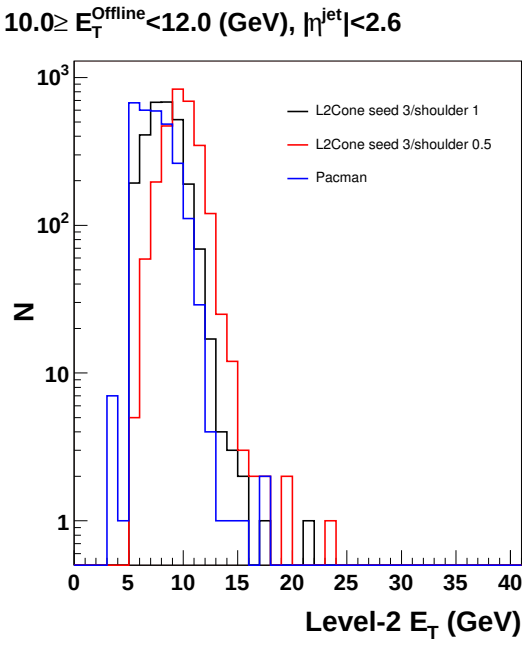

Figure 30: E_T distribution of L2Cones (*black*) and L2Clusters (*red*) corresponding to offline jets with E_T in the range $10 < E_T < 12$ GeV. (*left*) offline jets restricted to $|\eta| < 1.0$. (*right*) offline jets restricted to have no towers in the ROF $|\eta| > 2.6$.

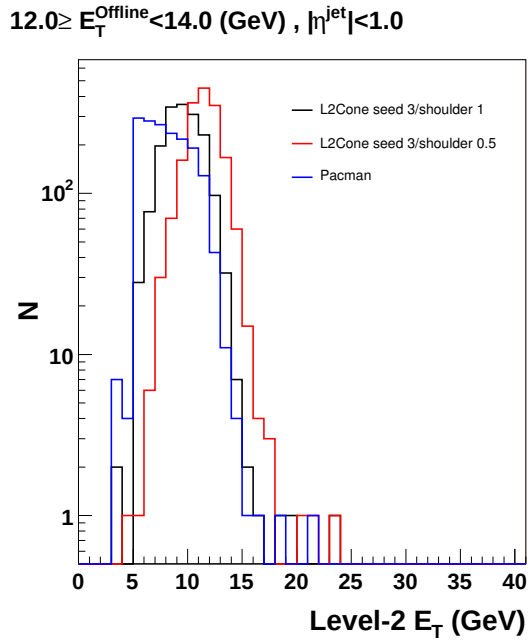

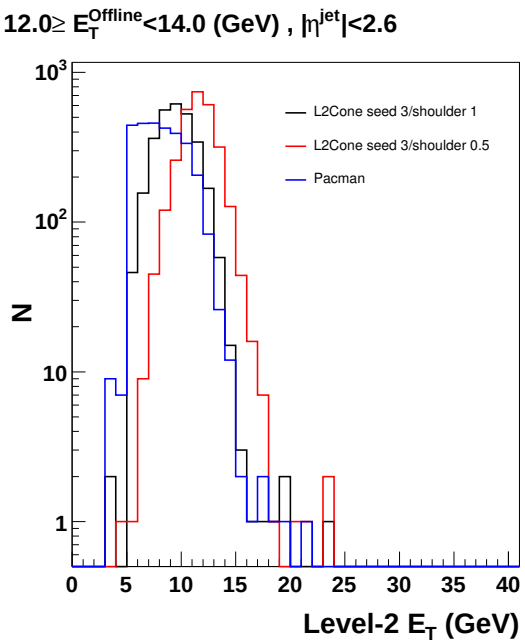

Figure 31: E_T distribution of L2Cones (*black*) and L2Clusters (*red*) corresponding to offline jets with E_T in the range $12 < E_T < 14$ GeV. (*left*) offline jets restricted to $|\eta| < 1.0$. (*right*) offline jets restricted to have no towers in the ROF $|\eta| > 2.6$.

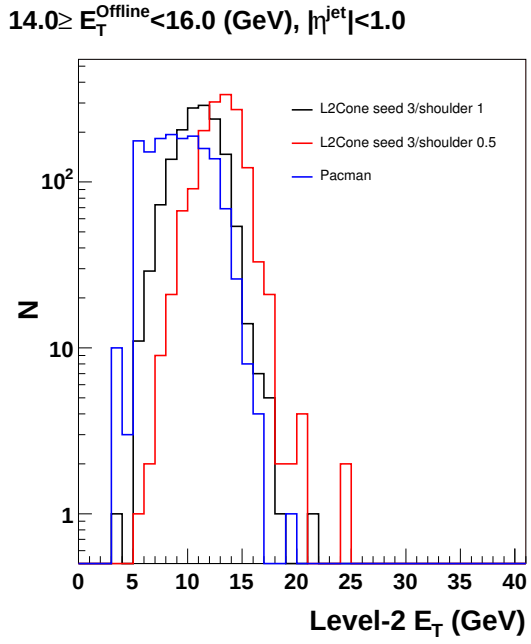

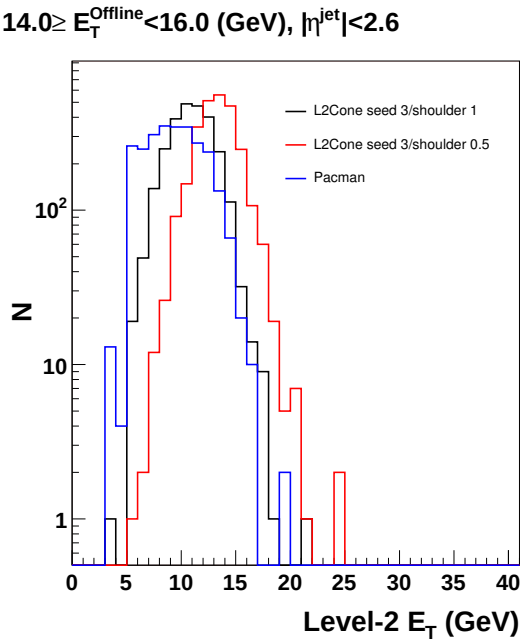

Figure 32: E_T distribution of L2Cones (*black*) and L2Clusters (*red*) corresponding to offline jets with E_T in the range $14 < E_T < 16$ GeV. (*left*) offline jets restricted to $|\eta| < 1.0$. (*right*) offline jets restricted to have no towers in the ROF $|\eta| > 2.6$.

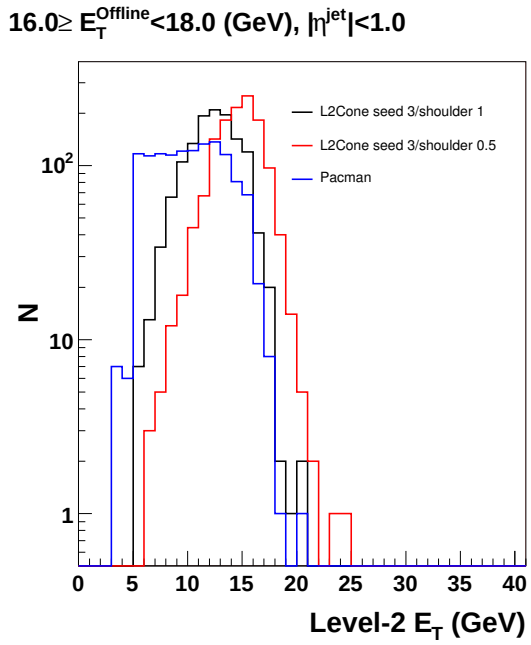

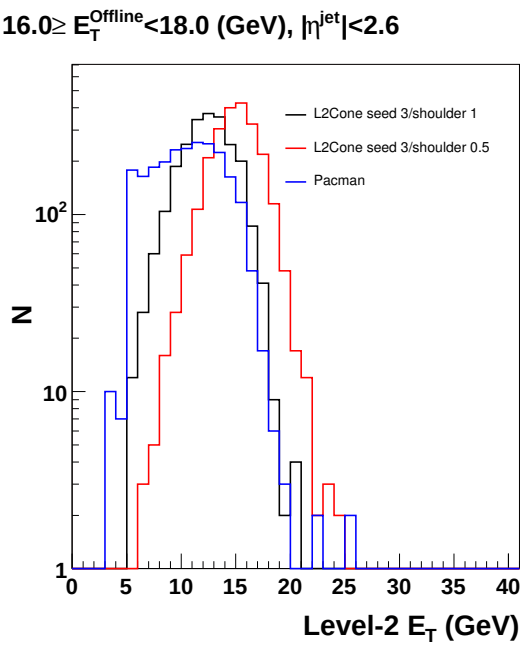

Figure 33: E_T distribution of L2Cones (*black*) and L2Clusters (*red*) corresponding to offline jets with E_T in the range $16 < E_T < 18$ GeV. (*left*) offline jets restricted to $|\eta| < 1.0$. (*right*) offline jets restricted to have no towers in the ROF $|\eta| > 2.6$.

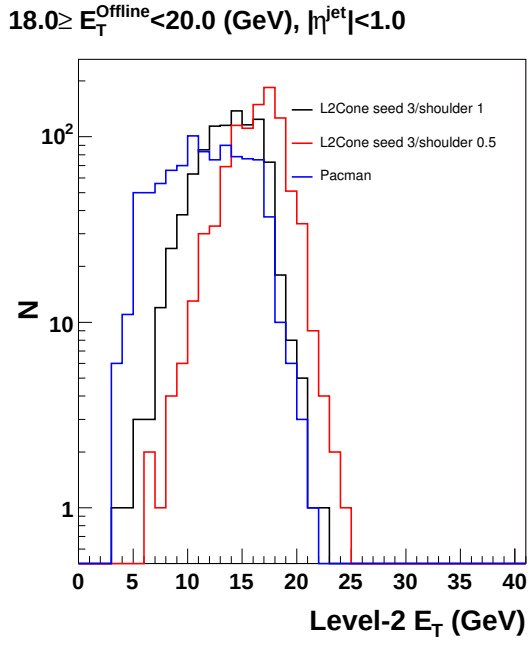

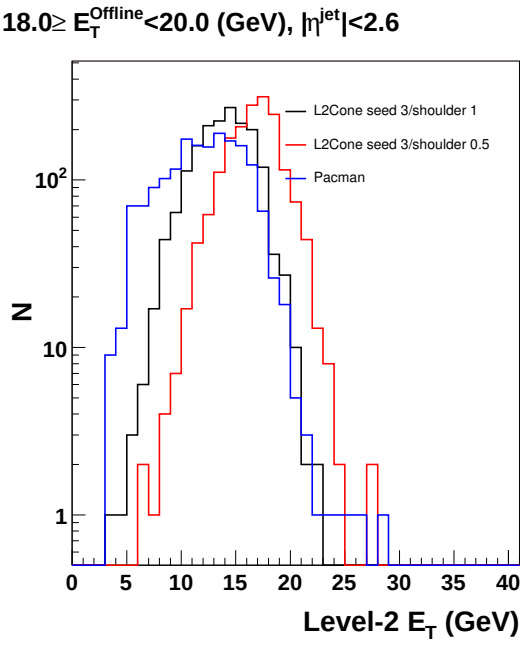

Figure 34: E_T distribution of L2Cones (*black*) and L2Clusters (*red*) corresponding to offline jets with E_T in the range $18 < E_T < 20$ GeV. (*left*) offline jets restricted to $|\eta| < 1.0$. (*right*) offline jets restricted to have no towers in the ROF $|\eta| > 2.6$.

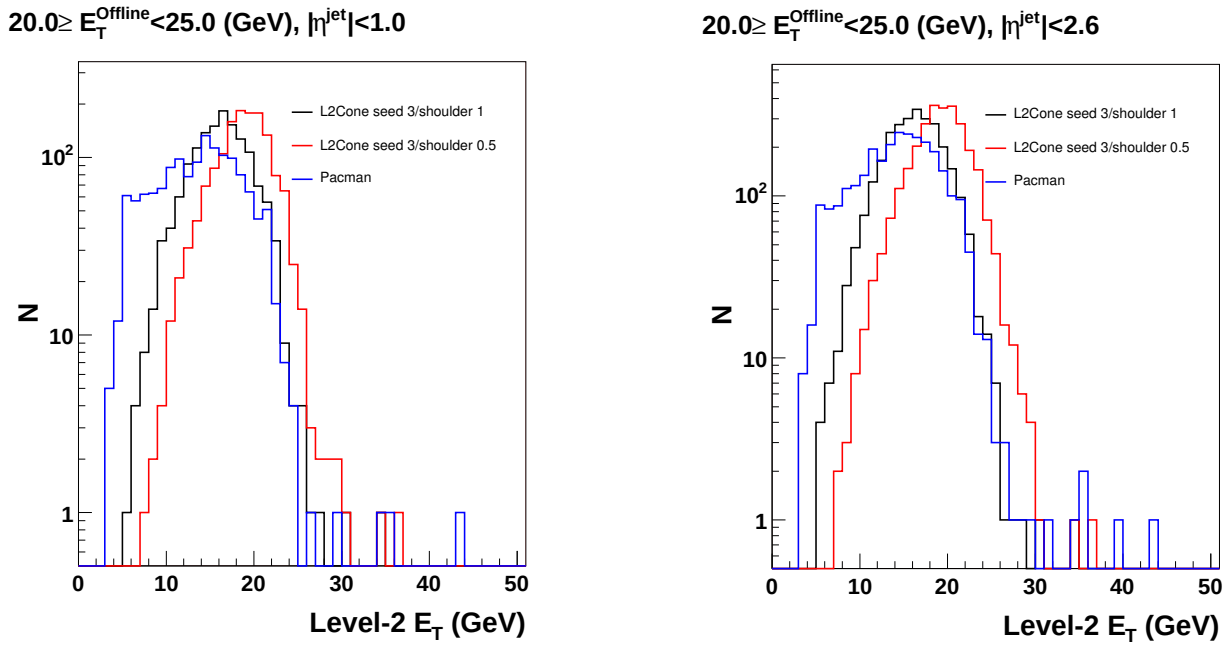

Figure 35: E_T distribution of L2Cones (*black*) and L2Clusters (*red*) corresponding to offline jets with E_T in the range $20 < E_T < 25$ GeV. (*left*) offline jets restricted to $|\eta| < 1.0$. (*right*) offline jets restricted to have no towers in the ROF $|\eta| > 2.6$.

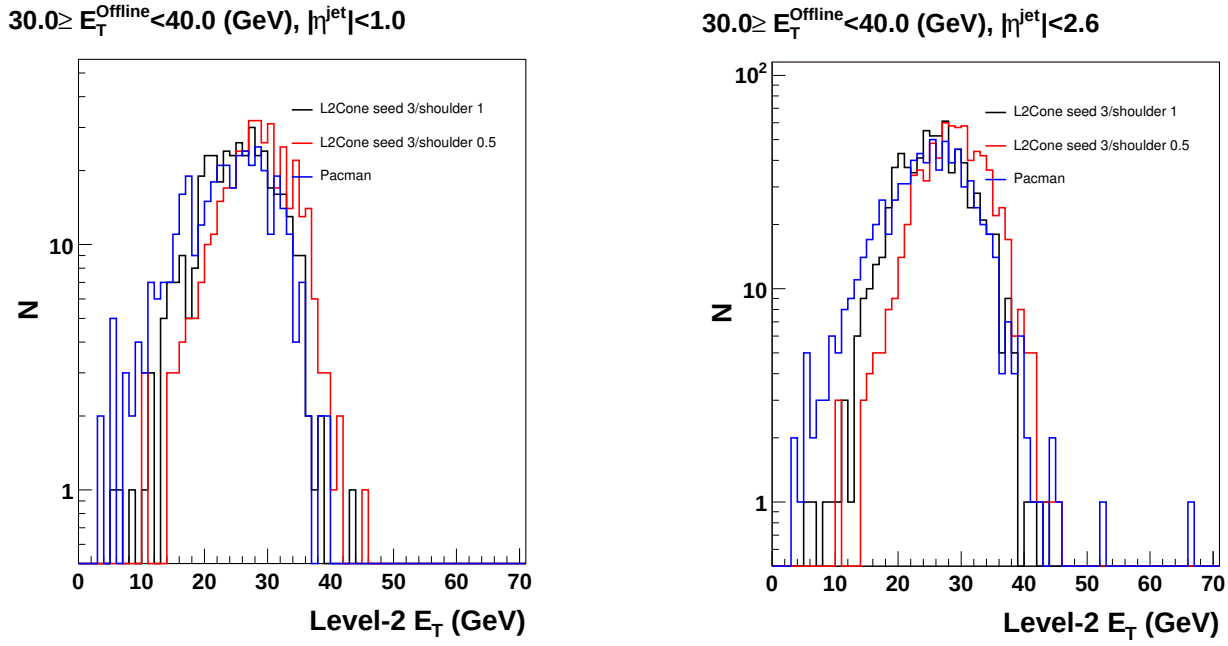

Figure 36: E_T distribution of L2Cones (*black*) and L2Clusters (*red*) corresponding to offline jets with E_T in the range $30 < E_T < 40$ GeV. (*left*) offline jets restricted to $|\eta| < 1.0$. (*right*) offline jets restricted to have no towers in the ROF $|\eta| > 2.6$.

3.1.3 Comparison of different thresholds for L2Cone

Figures 37-38 show results of the proposed L2Cone algorithm with seed and shoulder thresholds varying from 0, the ideal case where every tower can be considered a seed, to a seed threshold of 3 GeV and a shoulder threshold of 0.5 GeV, which may be favored due to timing constraints.

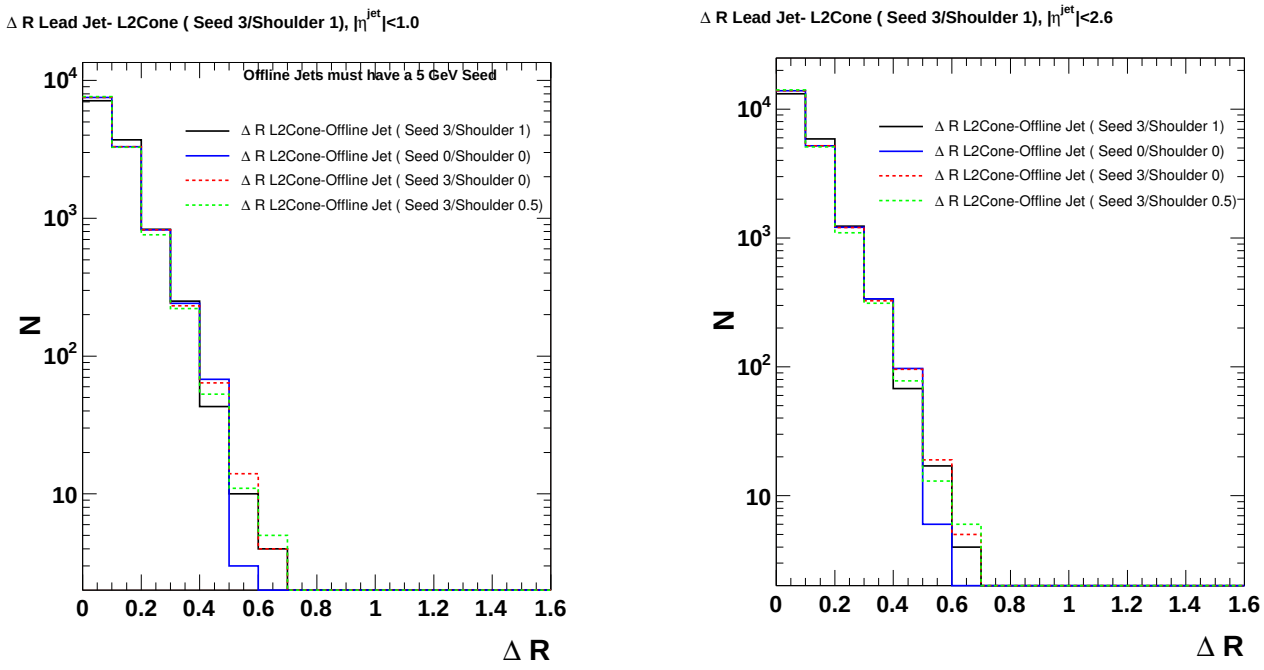

Figure 37: ΔR between leading jet and the matched L2Cone for varying seed and shoulder thresholds. (*left*) offline jets restricted to $|\eta| < 1.0$. (*right*) offline jets restricted to have no towers in the ROF $|\eta| > 2.6$.

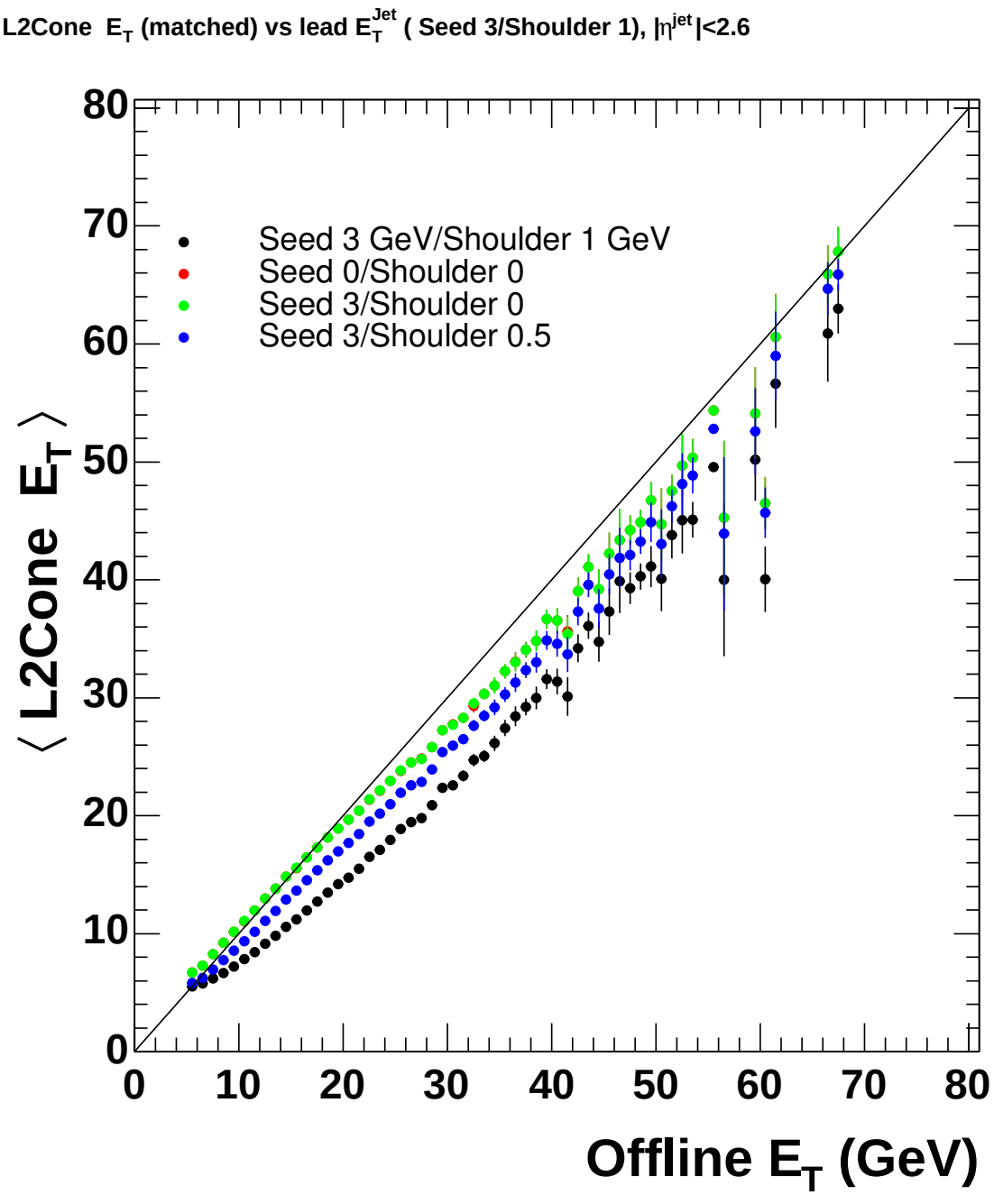

Figure 38: Correlation between L2Cone average E_T and leading offline jet E_T for varying seed and shoulder thresholds. The offline leading jet is required to have a 5 GeV L1 seed and is restricted to have no tower in the ROF $|\eta| > 2.6$.

3.1.4 Comparison of clustering performance including the effect of the Ring Of Fire

We also want to understand the consequences of the ROF removal from L2Clusters in the current trigger. The L2Cones have no restriction on the ROF, and a seed threshold of 3 GeV and a shoulder threshold of 3 GeV and 0.5 GeV is used. In the following plots, we do not restrict the η range of the offline jets, and look at up to four jets in the event, relevant for example, for multijet triggers. Figure 39 shows the efficiency for finding a L2Cluster or L2Cone within a radius of 0.7 of the offline leading jet (with a 5GeV confirming seed tower requirement), and Fig. 40 for the second-leading jet (with no 5GeV seed requirement). For the leading jet, we see that both L2 algorithms are 100% efficient, as expected with the 5GeV confirming seed tower, except for the L2Cluster when the offline jet is partially in the ROF. For the second-leading jet, we see similar matching efficiency for the L2Cones and L2Clusters except near the ROF region where the L2Clusters are very inefficient and where the L2Cones tend to find jets with even higher-E_T than reconstructed offline due to the extra activity in the ROF. This is also seen in the difference between L2 and offline E_T divided by offline E_T shown in Figs. 41-42. Figure 43 shows the correlation between average L2 E_T and offline jet E_T over the full η range for the leading jet up to the fourth-leading jet.

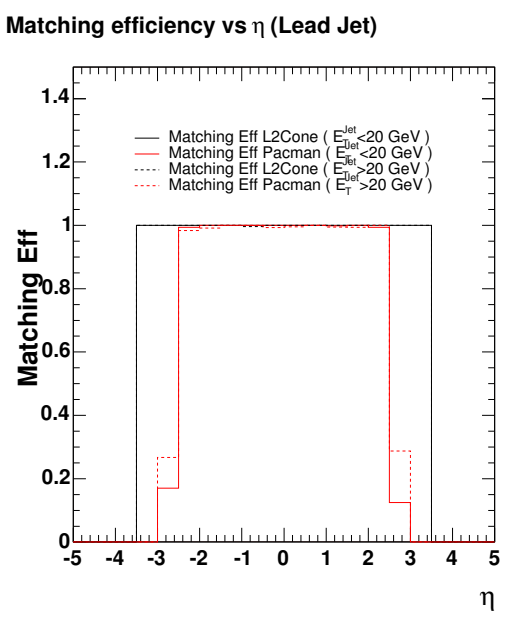

Figure 39: Efficiency for finding a L2Cone/Cluster within radius 0.7 of the leading offline jet (5GeV seed tower required) as a function of η. The inefficiency for L2Cluster (Pacman) at high η is due to the exclusion of towers in the Ring-Of-Fire. The efficiencies are plotted for offline jets with $E_T < 20$ GeV and $E_T > 20$ GeV.

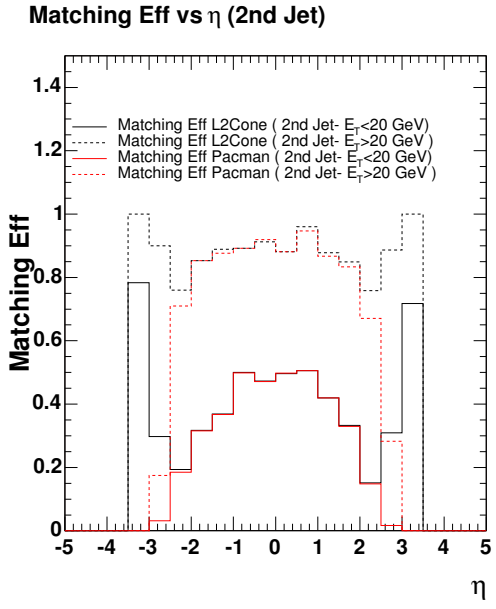

Figure 40: Efficiency for finding a L2Cone/Cluster within radius 0.7 of the second-leading offline jet (no 5GeV seed tower required) as a function of η. The inefficiency for L2Cluster (Pacman) at high η is due to the exclusion of towers in the Ring-Of-Fire, while the L2Cones become more efficient in that region due to the high ROF occupancy. The efficiencies are plotted for offline jets with $E_T < 20$ GeV and $E_T > 20$ GeV.

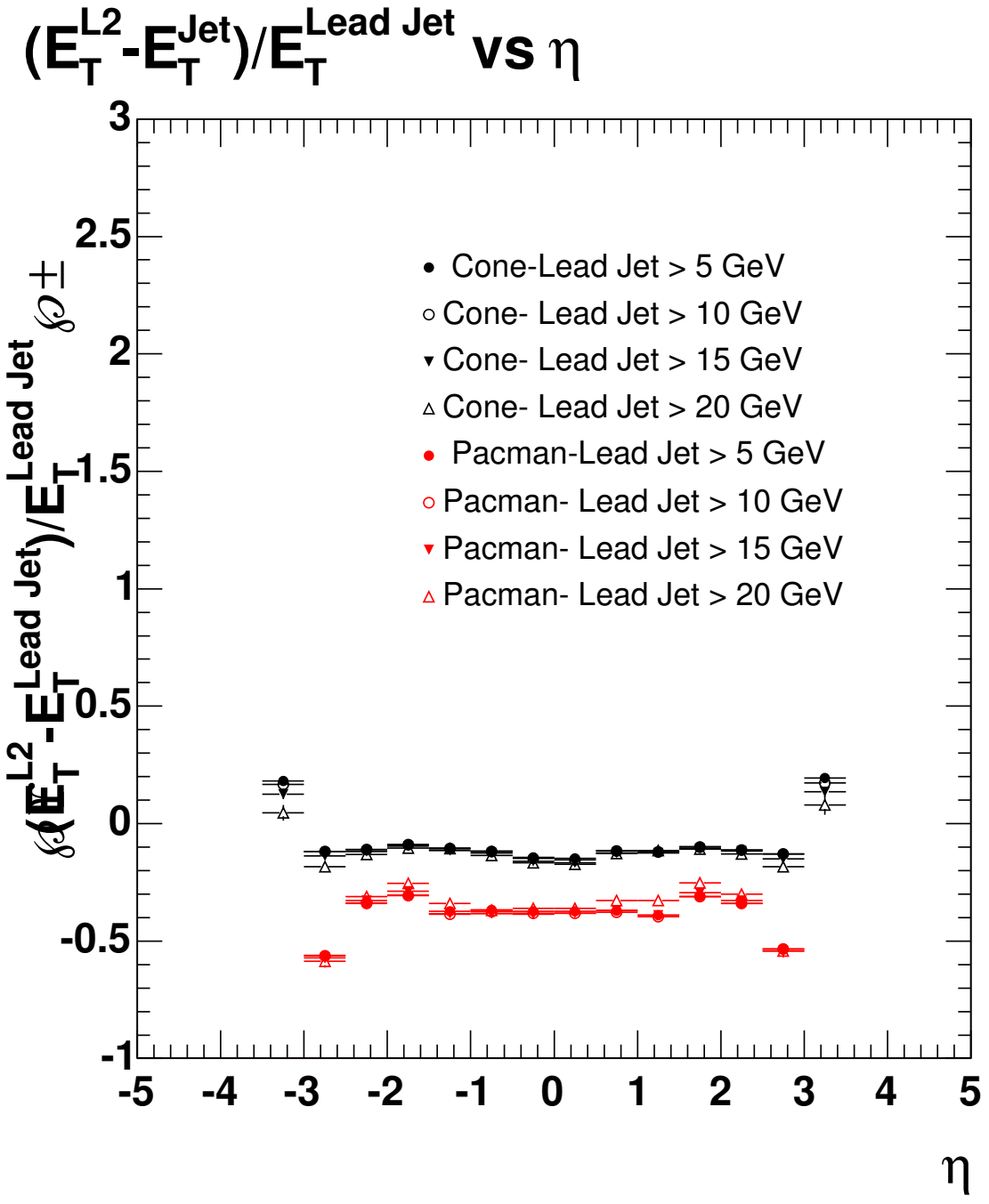

Figure 41: Relative fraction of leading offline jet E_T contained in the matched L2Cone/Cluster as a function of η for various E_T cuts. (The offline leading jet is required to have a 5GeV seed tower.) The inefficiency for L2Cluster (Pacman) at high η is due to the exclusion of towers in the Ring-Of-Fire, while the L2Cones become more efficient in that region due to the increased ROF activity.

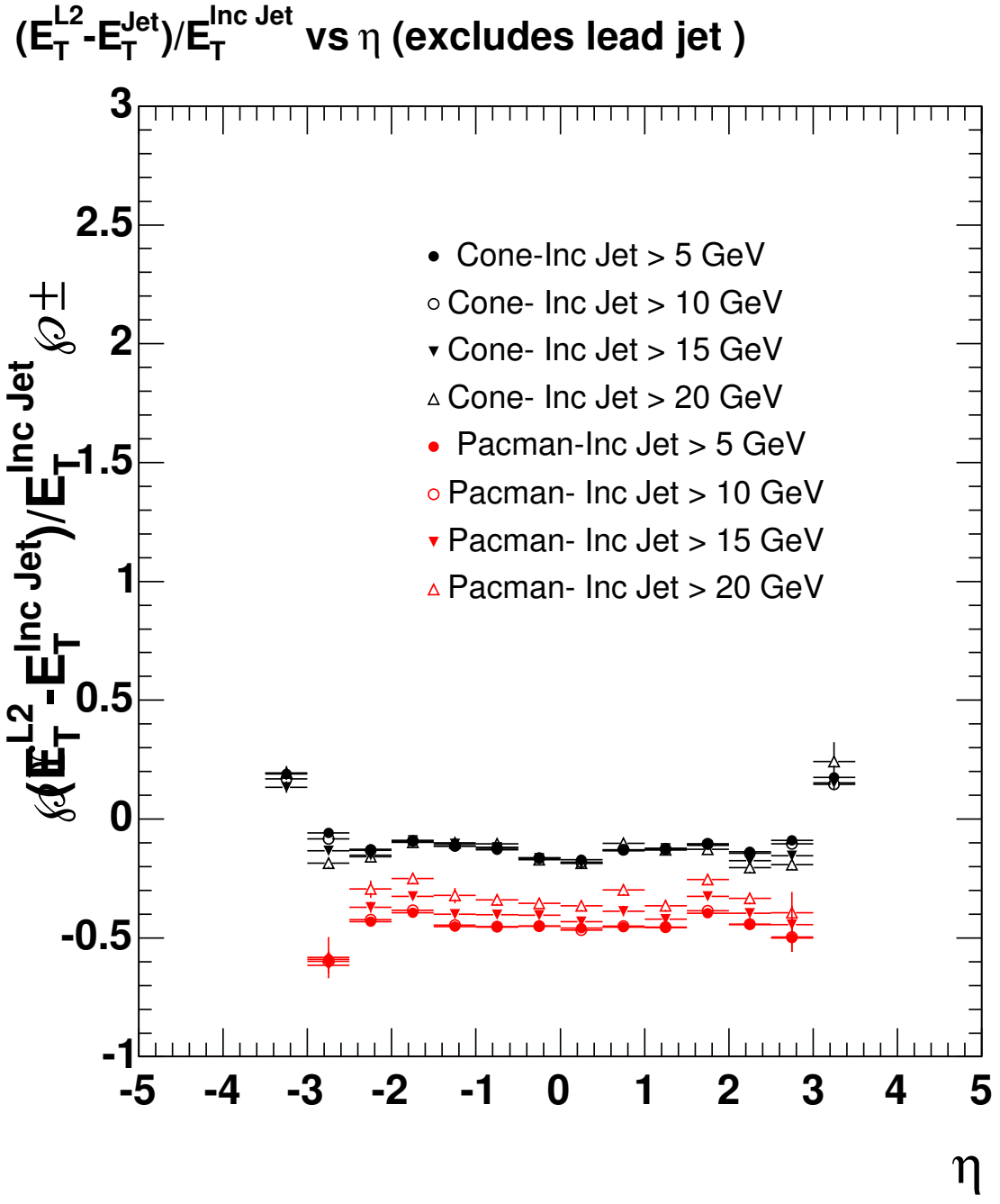

Figure 42: Relative fraction of non-leading offline jet E_T contained in the matched L2Cone/Cluster as a function of η for various E_T cuts. (The jets are not required to have a 5GeV seed tower.) The inefficiency for L2Cluster (Pacman) at high η is due to the exclusion of towers in the Ring-Of-Fire, while the L2Cones become more efficient in that region due to the increased ROF activity.

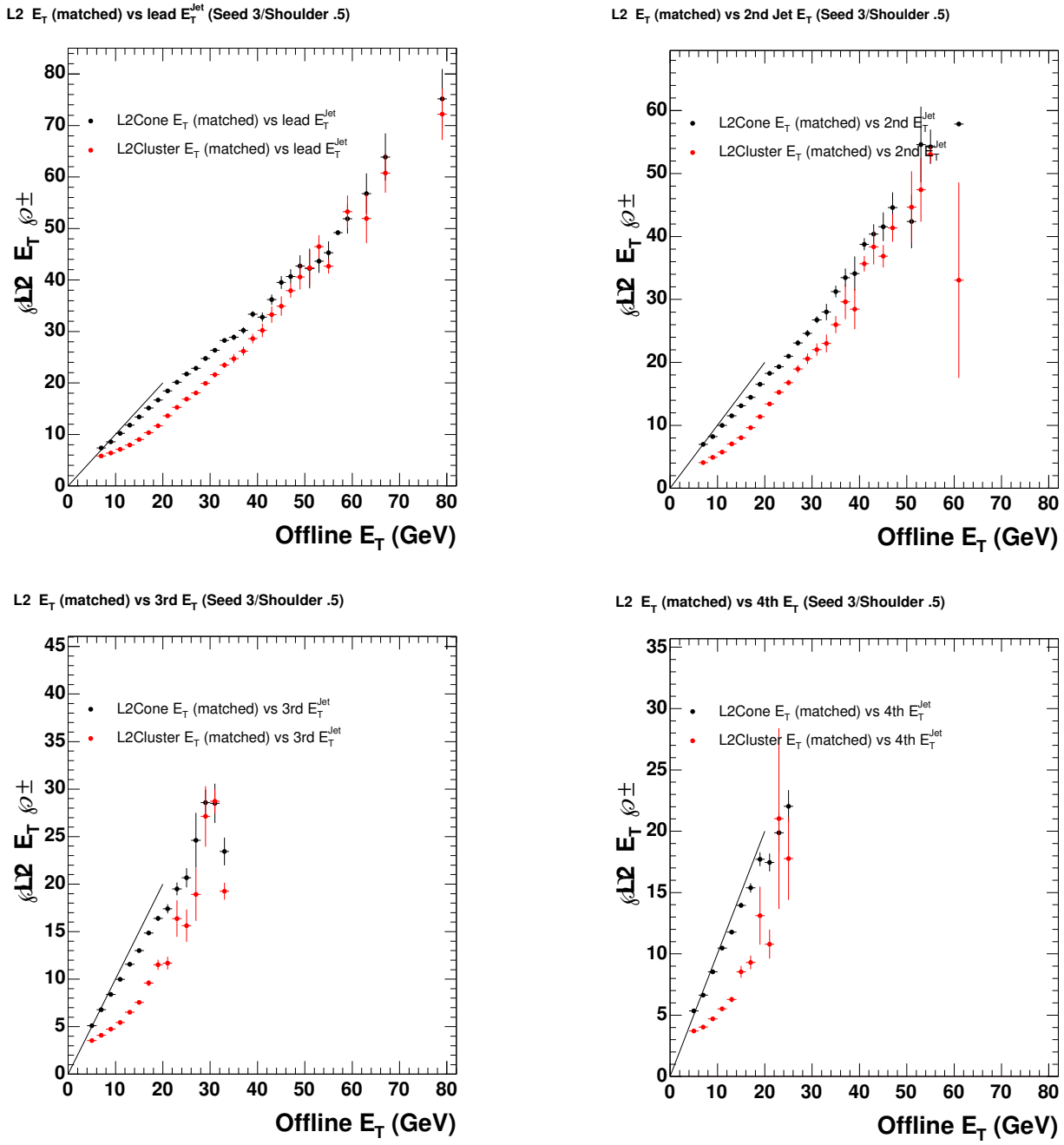

Figure 43: Correlation between mean L2Cone/Cluster E_T and offline jet E_T for the first through fourth leading offline jets. (The leading jet is required to have a 5GeV seed tower, but the non-leading jets are not.)

3.1.5 L2 jet trigger efficiencies and rates

In this section, we will study the impact of the upgrade on the trigger efficiency and purity for the inclusive jet triggers. The inclusive jet triggers are used in QCD analyses, jet energy and resolution studies, b-tagging studies, and as backup triggers for many important high-p_T physics analyses. The effect of the proposed L2Cone algorithm on these trigger cross sections will also give an indication of the effect on more exclusive triggers requiring jets. The jet triggers require

- Level-1: Single tower with $E_T \geq 5$, (5), 10, 20 GeV. They drive:
- Level-2: A single cluster with $E_T \geq 15$, 40, 60, 90 GeV respectively, which in turn drive:
- Level-3: A single jet with $E_T \geq 20$, 50, 70, 100 GeV, respectively.

All of these trigger paths have L2 cross sections that grow with increasing luminosity. Using the proposed L2Cone algorithm reduces the growth rate since the fixed cone clustering is much less sensitive to the effect of high occupancy than the current L2Cluster algorithm. In the histograms of number of towers which make up the L2 jets shown in Fig. 44, the "Pac-man" nature of the L2Cluster algorithm is seen for 40 GeV clusters in the second peak at > 20 towers in a cluster. The L2Cone algorithm limits the number of possible towers included.

In order to compare the efficiency for both algorithms, we first define the current L2Cluster trigger efficiency as the ratio of the events with a 20 GeV jet and a L2Cluster with $E_T \geq 15$ GeV divided by the parent sample (events with a 20 GeV jet). We then replace the L2Cluster requirement with a L2Cone requirement and scan the cut values to find the L2Cone E_T cut that reproduces the L2Cluster efficiency. A similar procedure is used for the higher-E_T jet triggers. For these studies, a seed (shoulder) threshold of 3 (0.5) GeV is used for the L2Cones. The trigger efficiencies for Jet20, Jet50, and Jet70 are shown in Fig. 45.

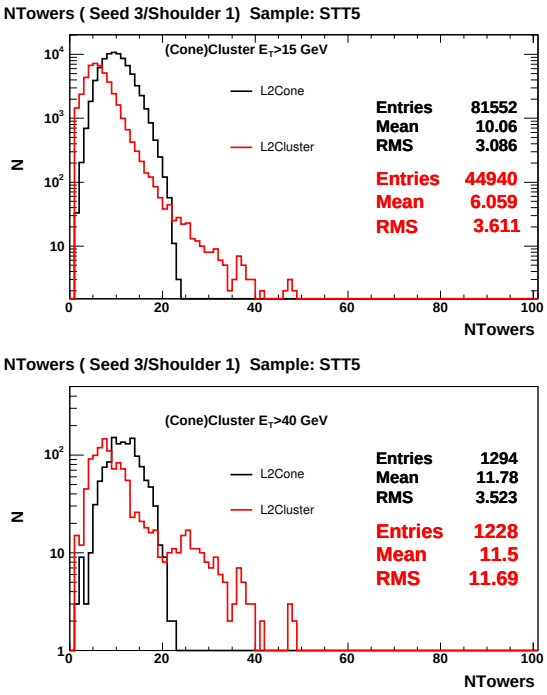

Figure 44: Number of towers which make up the L2Cones (*black*) and L2Clusters (*red*) with L2 threshold of $E_T > 15$ GeV (*top*) and $E_T > 40$ GeV (*bottom*). The ROF is excluded from clustering for both L2Cluster and L2Cone.

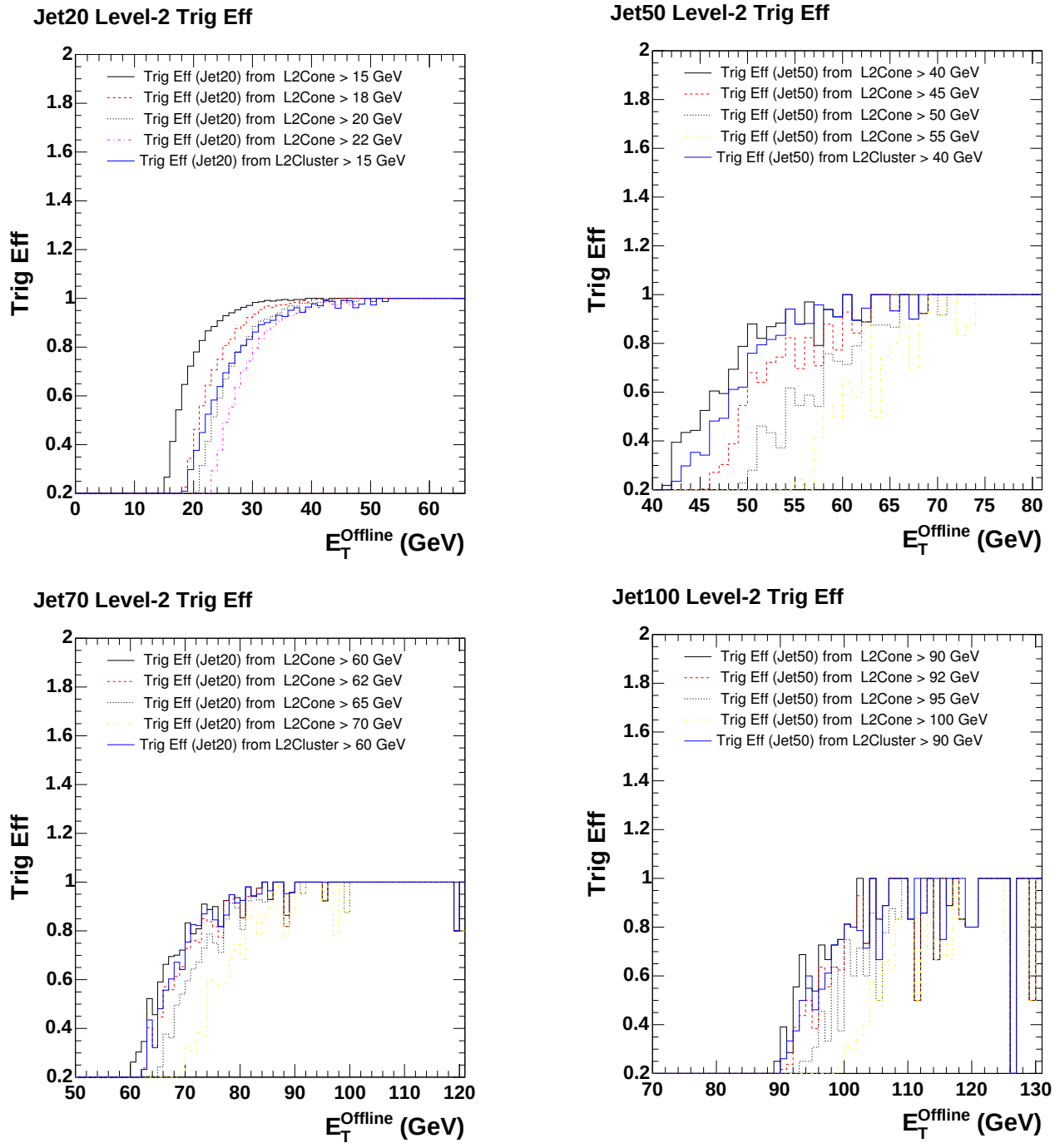

Figure 45: Level-2 jet trigger efficiencies for a spread of L2Cone E_T thresholds and also for L2Cluster with the default E_T thresholds. L2Cones include the ROF while the L2Clusters do not.

We want to quantify how the L2 rate will change when the current L2Cluster algorithm is replaced by the proposed L2Cone algorithm. To determine the effect on the growth of the rate with instantaneous luminosity, we do the following:

- Select STT5 events with at least one jet with $E_T \geq 5$ GeV.
- Find the L2Cone cut that reproduces the current L2Cluster trigger efficiency (Fig. 45). For the Jet20 trigger efficiency, the L2Cone cut is 20 GeV (the current L2Cluster cut is 15 GeV). For Jet50, it is 40 GeV (the same as the current L2Cluster cut).
- Look at the fraction of the STT5 events that have a L2Cone that satisfies the cut above and also an offline jet with $E_T \geq 20$ GeV (50 GeV) for Jet20 (Jet50).
- Look at the fraction of the STT10 events that have a L2Cone that satisfies the cut of 60 (90) GeV and also an offline jet with $E_T \geq 70$ GeV (100 GeV) for Jet70 (Jet100).

Changing from the existing L2Cluster algorithm to the proposed L2Cone algorithm, we see in Fig. 46 that although the growth of the Jet20 rate as a function of instantaneous luminosity is about the same, the overall rate is reduced due to the fact that a higher L2 threshold can be used. For Jet50 there is a significant improvement in the growth rate; Jet70 and Jet100 show improvement as well.

We are likely seeing that the low- and high-E_T jet samples are sensitive to pile-up in different ways. The low-E_T jet triggers tend to select soft events, and the rate increase is sensitive to pile-up moving all the jets to higher energy, increasing the probability that a jet is over the threshold and will trigger the event. The high-E_T jet triggers appear to be more sensitive to pile-up causing a merging of towers to produce large fake clusters during the clustering. The proposed fixed-cone algorithm is much less sensitive to this effect than the current clustering algorithm.

Figure 46 also shows that the ROF cut may no longer be necessary with the L2Cone algorithm.

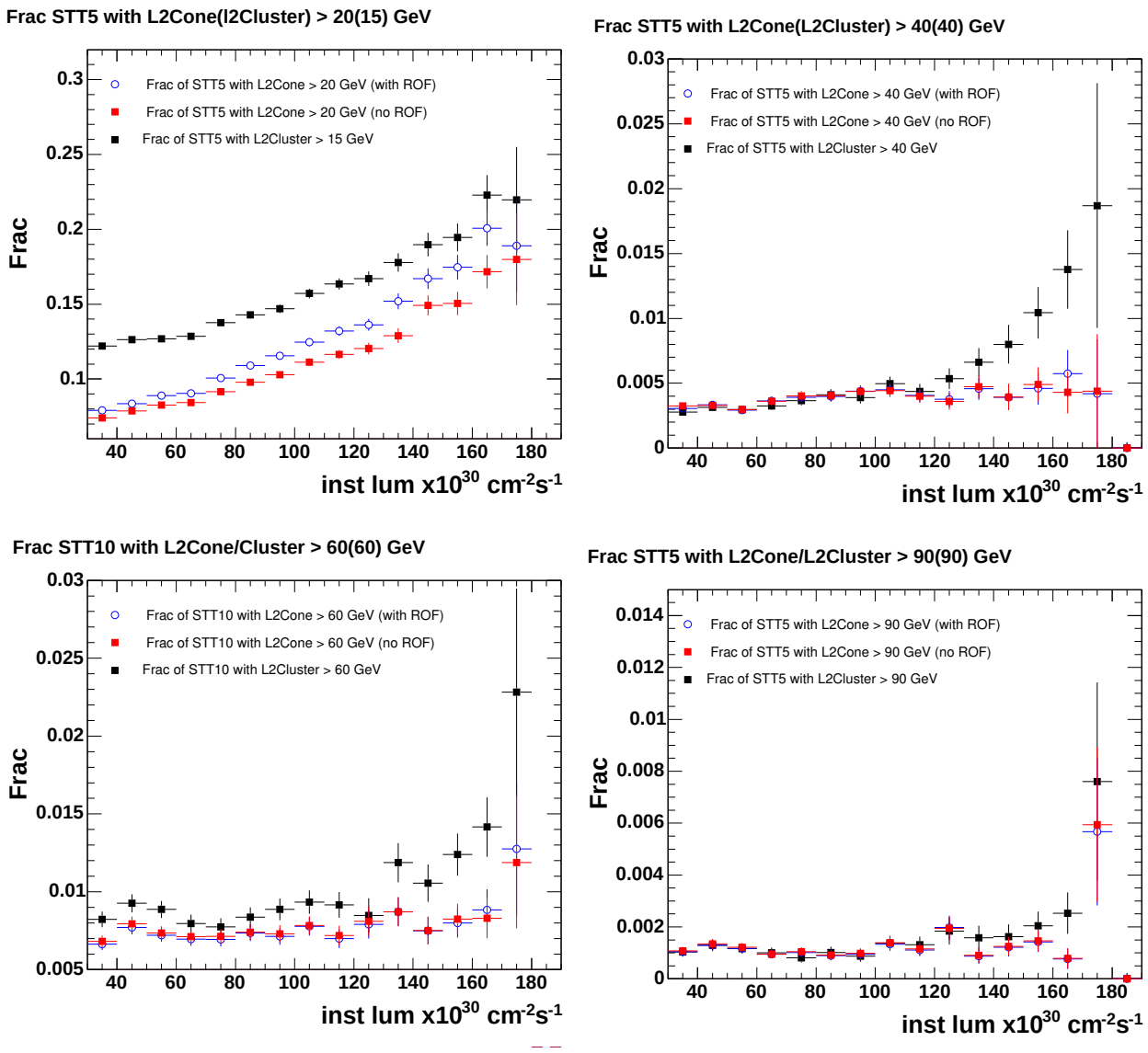

Figure 46: Fraction of STT5/STT5/STT10/STT10(20) events with a L2Cone E_T $\geq$22/40/60/90 GeV and also for L2Cluster E_T $\geq$15/40/60/90 GeV. For L2_JET40, significant improvement in the growth rate is attained by using L2Cone. L2_JET60 and L2_JET90 are more well-behaved at lower luminosities due to the higher L1 thresholds required, but they show improvement from using L2Cone as well, which will be significant at higher instantaneous luminosity. Also shown is the effect of allowing towers from the Ring-of-Fire (ROF) to be included in the L2Cones; the cross section grows with luminosity for 20 GeV L2Cones, but there is little effect on the higher E_T triggers.

3.1.6 L2 missing-E_T rates

There are several possible Higgs searches that make use of the MET+jets signature, two examples are $ZH \to \nu\nu bb$ and $WH \to l\nu bb$. The signal has a distinctive topology of large missing E_T and 2 jets, one of which is b-tagged offline. The trigger used for these searches is:

- Level-1: missing $E_T > 25$
- Level-2: 2 jets
- Level-3: missing $E_T > 35$

This trigger has a L2 cross section that grows very rapidly as instantaneous luminosity increases; after the L3 requirement the cross section becomes much more manageable in both overall size and growth with instantaneous luminosity (see Fig 2). The upgrade we propose would introduce the full calorimeter trigger tower information at Level 2. Then an additional requirement of $\not\!\!E_T > 35$ can be introduced earlier which would suppress the rate growth to something more like we currently see at Level 3. In addition, it may be possible to use the $\Delta\phi$ between the $\not\!\!E_T$ and the second jet to reduce the QCD background (where $\not\!\!E_T$ is aligned with a jet) in the Higgs/SUSY triggers.

The L2 MET is calculated from the 10-bit trigger tower E_T information taking ϕ as the value of the tower center. The $\not\!\!E_T$ angle ϕ_{MET} can also be determined. Figure 47 shows the difference between L1 MET (currently not improved at Level 2) and offline MET. Figure 48 shows the difference between the MET calculated at Level 2 as described above and the offline MET.

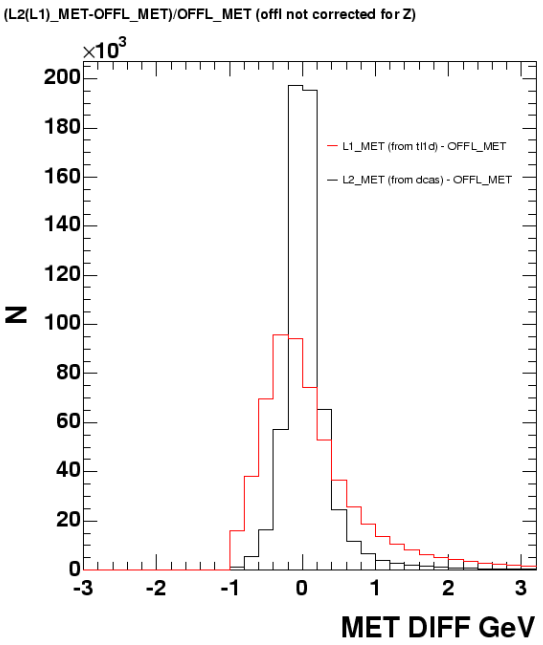

Figure 47: $(\not\!\!E_T^{\mathrm{L1}} - \not\!\!E_T^{\mathrm{offl}})/\not\!\!E_T^{\mathrm{offl}}$ (current) and $(\not\!\!E_T^{\mathrm{L2}} - \not\!\!E_T^{\mathrm{offl}})/\not\!\!E_T^{\mathrm{offl}}$ (proposed).

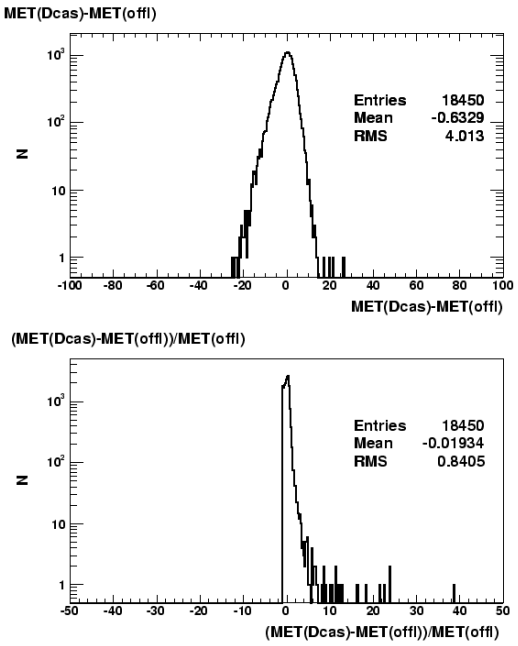

Figure 48: (*top*) $\not\!\!E_T^{\mathrm{L2}} - \not\!\!E_T^{\mathrm{offl}}$, (*bottom*) $(\not\!\!E_T^{\mathrm{L2}} - \not\!\!E_T^{\mathrm{offl}})/\not\!\!E_T^{\mathrm{offl}}$.

In order to study the effect of the proposed upgrade on the MET25 and MET35_2JET10 triggers, the following was done:

1. Begin with the STT5 sample, as this should introduce negligible bias and also provide enough statistics for events with MET>25(35) GeV.
2. Find the fraction of the sample that pass MET> 25 (L1) as a function of instantaneous luminosity.
3. Find the fraction of the sample that pass MET> 25 (L1) and have two L2Clusters with $E_T > 10$ as a function of instantaneous luminosity.
4. Instead of using L1 MET at Level 2, recalculate the MET from DCAS towers and apply a L2 cut of 35 GeV (the current L3 cut).
5. Finally replace L2Clusters with the proposed L2Cones.

By using this L2 MET, we see in Fig. 49 that the growth term in the trigger rate is suppressed and now looks much more like what is seen at Level 3. Although the use of the proposed L2Cones in this trigger do not contribute much to the rate reduction, they may be very useful when used in conjunction with the ϕ_{MET} in filtering out some of the QCD backgrounds.

Figure 49 also shows results when the study is repeated using a L2 MET threshold of 30 or 25 GeV in order to investigate whether the increased precision of the MET calculation would allow relaxed cuts on MET. Figure 50 shows the effect on the MET+2JET trigger of lowering the L1 requirement of to $\not\!\!E_T$ >15 GeV for varying L2 requirements of $\not\!\!E_T > 15$, 20, and 25 GeV.

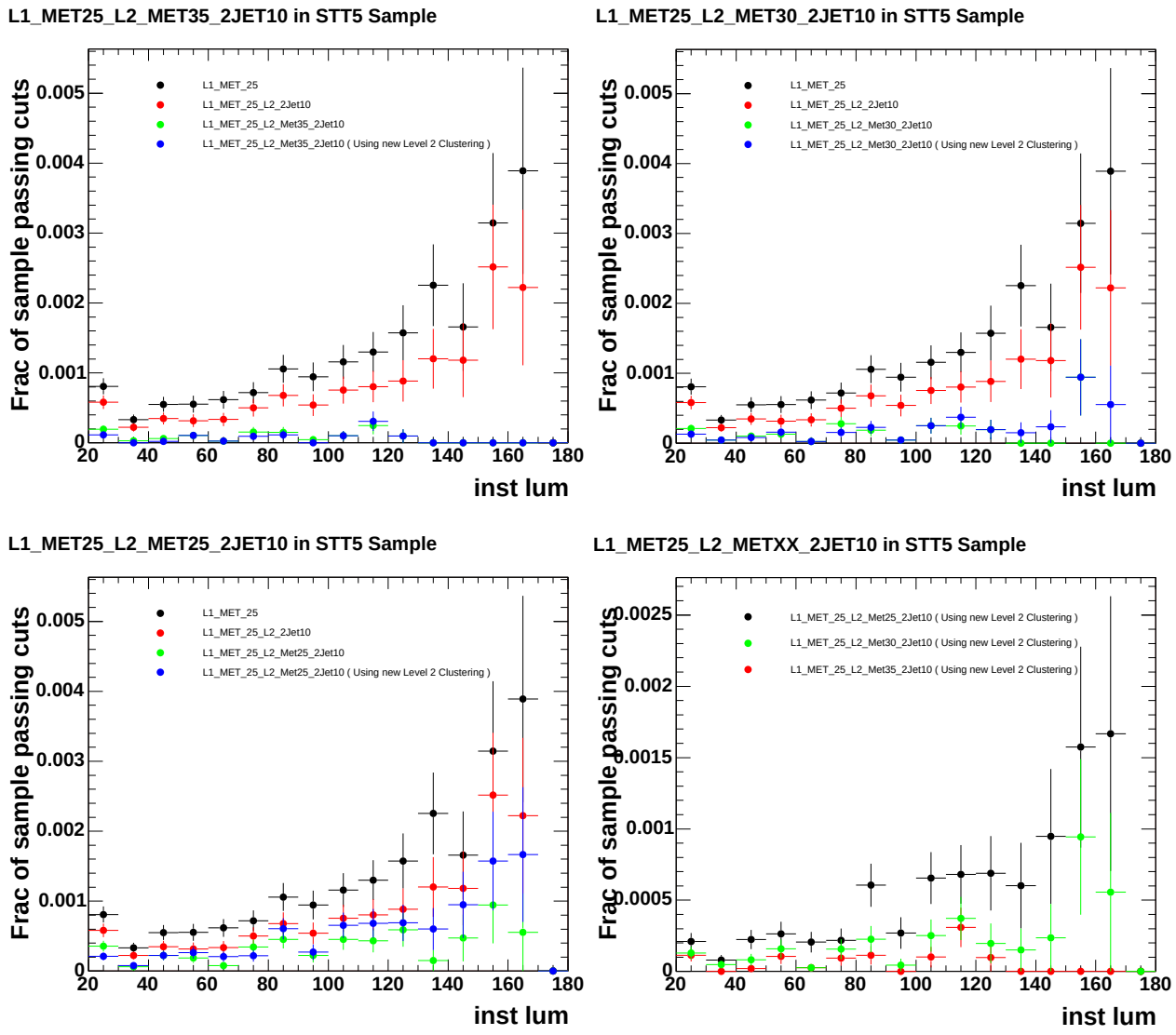

Figure 49: Fraction of events in the STT5 sample that pass increasingly tighter cuts, in order to investigate the effect of the L2CAL upgrade on the MET+2JET trigger path. First, MET25 is required at Level 1 (*black*). Then a L2 requirement of two 10 GeV L2Clusters is applied to mimic the current L2CAL performance (*red*). Next, a cut on the MET recalculated at L2 using the higher-precision information provided by the L2CAL upgrade is applied (*green*). The different plots are made requiring different values of this L2 MET: MET35, MET30, and MET25. Finally, the effect of using the new L2Cone is shown (*blue*). The varying L2 MET requirements are compared more closely in the *lower-right* plot.

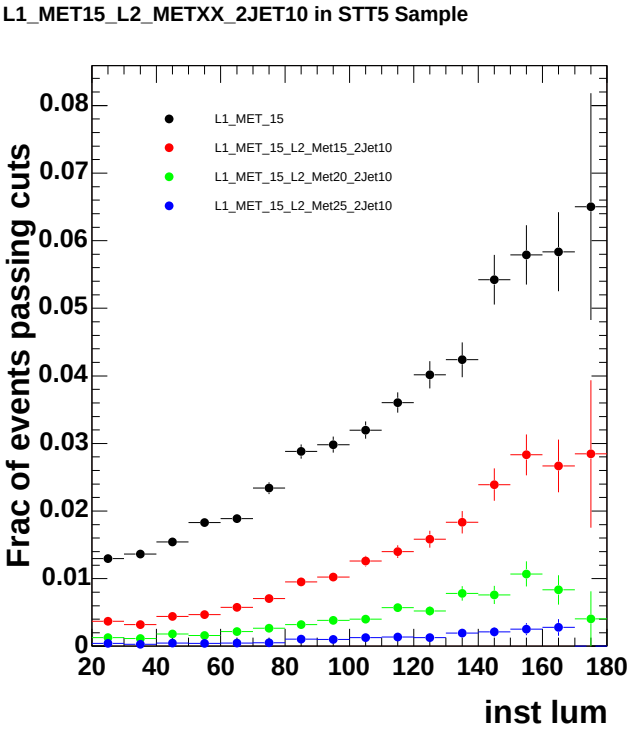

Figure 50: Fraction of events in the STT5 sample that pass increasingly tighter cuts, in order to investigate whether the L2CAL upgrade allows a looser MET cut at Level 1 of 15 GeV for the MET+2JET trigger path. L1_MET15 is required first (*black*), then two 10 GeV L2Cones along with varying L2 requirements of MET25 (*red*), MET20 (*green*), and MET15 (*blue*).

Figure 51 shows the effect on the growth rate of the inclusive L1_MET_25 trigger when L2 MET cuts of 35, 30, and 25 GeV are imposed. Figure 52 is a similar plot for reduced L1 and L2 thresholds: L1_MET_15 trigger when L2 MET cuts of 25, 20, and 15 GeV are imposed.

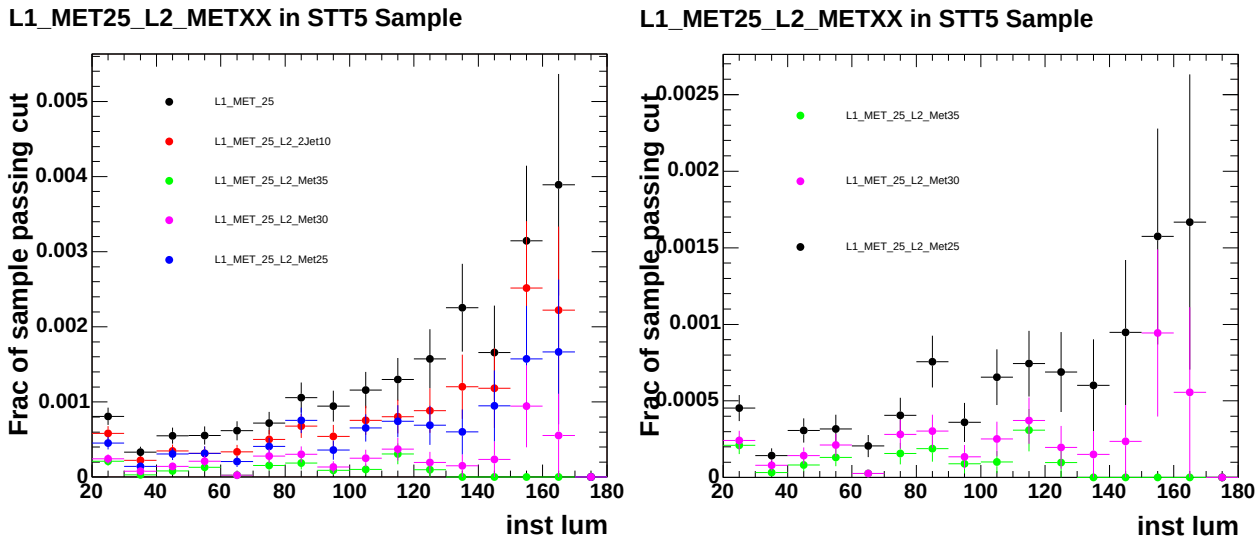

Figure 51: Fraction of events in the STT5 sample that pass: L1_MET_25 and L2_METXX for varying L2 requirements of MET35, MET30, and MET25 .

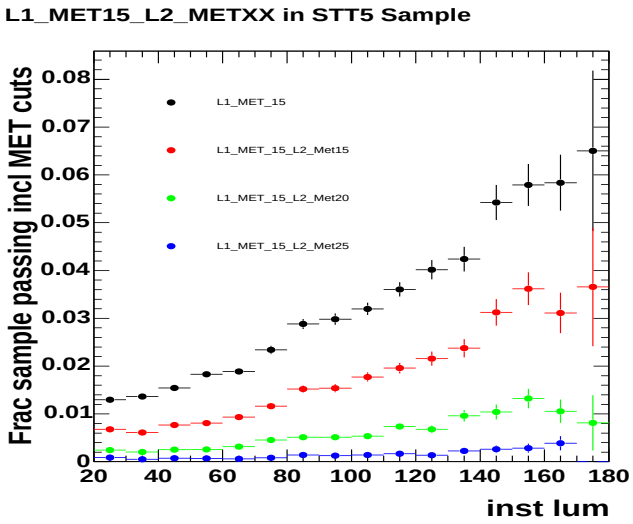

Figure 52: Fraction of events in the STT5 sample that pass: L1_MET_15 and L2_METXX for varying L2 requirements of MET25, MET20, and MET15 .

3.2 Timing study

In this section we present the status and plans of the timing studies for the proposed Level-2 clustering and $\not\!\!E_T$ algorithm.

In principle, the proposed clustering and $\not\!\!E_T$ calculation could be done separately. However, it is somewhat natural to include the $\not\!\!E_T$ calculation in the same algorithm since the inclusion is straightforward and makes use of some of the clustering code that already exists. Also, combining the two calculations in the same software allows easy access to quantities such as $\Delta\phi$ between the L2Cones and the $\not\!\!E_T$.

We assume as input for the algorithm all the non-zero E_T towers. For each input tower, η, ϕ, and the Had and Em E_T are provided. The algorithm performs the following steps:

1. Sum Em and Had energy for each tower, selecting seeds and shoulders according to threshold (3 GeV for seeds and 0.5 GeV for shoulders).
2. $\not\!\!E_T$ calculation. (This operation could be done while looping over all the input towers for the previous item.)
3. Sort the seed list in decreasing E_T.
4. L2cones generation. Beginning with the first seed: sum the E_T of all the towers above the shoulder threshold (which allows seed towers to also be used in a L2Cone) in a cone of $R = 0.7$ of the seed. The shoulders around the seed are directly addressed by using a look-up table (to speed up the algorithm). Mark all towers used in the current L2Cone as *used* and then move to the next seed tower in the list that is not marked as *used* and repeat. When seed tower list is exhausted return a list of the first 20 L2Cones.
5. Sort the L2Cone list in decreasing E_T.

Note that we have not added the isolation algorithm, and the two electron passes, in the timing study. We expect that we will run these existing algorithms in the L2 decision CPU as well. Work is in progress to include these algorithms; we expect the extra CPU time taken to be negligible since they are simpler than the cluster finding.

3.2.1 Method

In order to test the algorithm speed, we stripped out the DCAS tower information for several events. The data samples/events are as follows:

- DCAS strip JET100 (instantaneous luminosity in the range 120-170 $\times 10^{30}$ cm^{-2}s^{-1}).
- DCAS strip JET100 plus minimum bias

We use an AMD Opteron processor for the L2Cone clustering algorithm timing study (in fact, it is the spare L2 decision PC). We set the maximum priority for the algorithm on one of the CPU's and tie all other resources for system operations, such as interrupt operations,

to the second CPU. The processor and settings are the same as we are using in the system for the L2 decision PC.

As a preliminary estimate for the time to run the algorithm we did the following (note this is the same method as was used to estimate the L2 algorithm CPU time for the L2 Pulsar upgrade of the L2 decision crate):

- Built a stand-alone version of the clustering code and hard coded in the DCAS tower information.
- Constructed the inputs to the clustering algorithm; this includes creating a C++ structure that stores for each DCAS tower the Em, Had, η and ϕ.
- Begin the clock.
- Run the clustering algorithm and MET calculation.
- Stop the clock.

The clock set up was as follows:

```
#include <stdlib.h>
#include <unistd.h>
#include <stdio.h>
#define rdtscl(low) \
__asm__ __volatile__ ("rdtsc" : "=a" (low) :: "edx")
#define CLOCKS_PER_USEC 2330.813
#define NUM_EVENT=150
unsigned long num, start[NUM_EVENT], end[NUM_EVENT]
for(int iev=0;iev<NUM_EVENT;iev++){
rdtscl(start[iev]);
Do clustering here on event iev
rdtscl(end[iev]);
float TimePerEvt = (float)(end[iev]-start[iev])/CLOCKS_PER_USEC;
```

3.2.2 Results

Figure 53 reports the code execution time (including the $\not\!\!E_T$ calculation, jet clustering, and sorting) for events from a sample of 350 Jet100 events taken with $\mathcal{L}$ ∼(120-170) $\times 10^{30}$ $\mathrm{cm}^{-2}\mathrm{s}^{-1}$, and Figs. 55 and 54 show the code execution time vs. the instantaneous luminosity and number of vertices, respectively. The mean execution time is ∼6.5μs, going as high as ∼10μs in events with 10 vertices. Fig. 56 reports the execution time for 1500 events created by merging an event from the Jet100 sample with an event from a minimum bias sample, which has a mean of ∼9.5μs and goes as high as ∼ 20μs. Together with a transfer latency less than 10μs on average, the maximum latency for the new L2CAL path would be within ∼30μs. This is already very good. Note that the average SVT latency is ∼30μs with a long tail, yet we can still run the L1 accept at 30kHz with ∼10% deadtime.

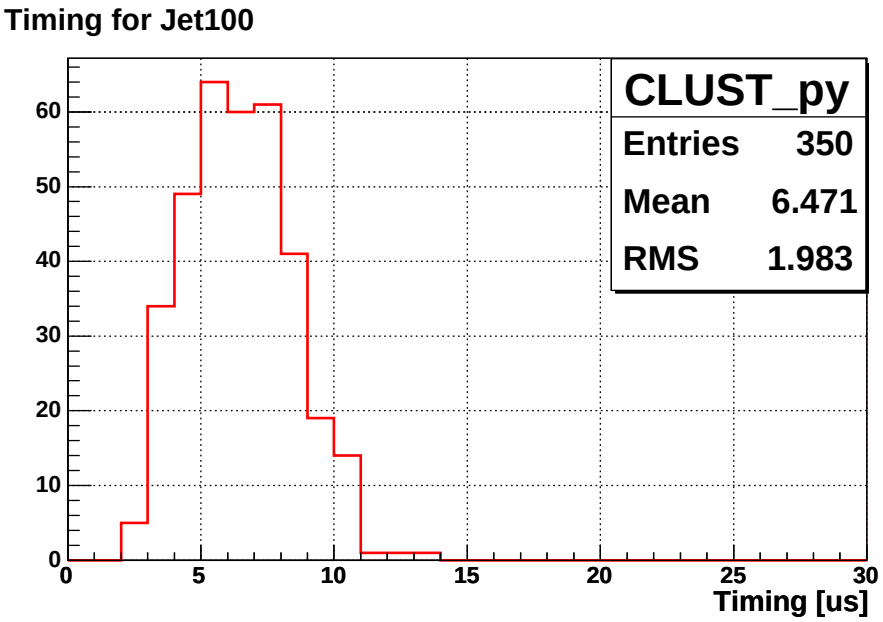

Figure 53: Code execution time for Jet100 sample.

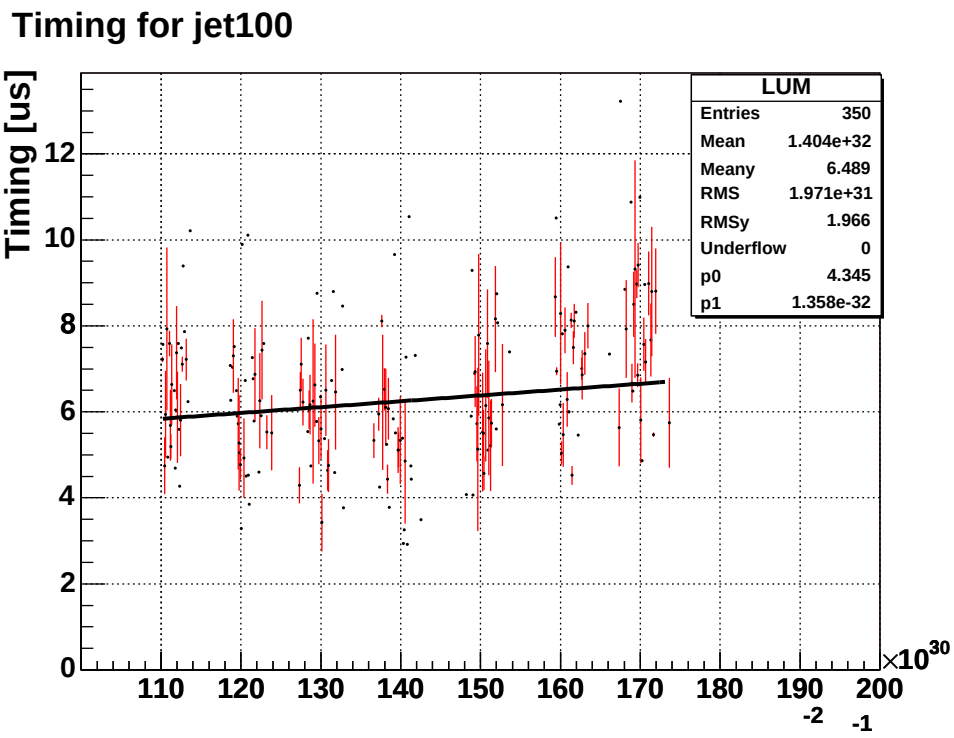

Figure 54: Clustering execution time as function of luminosity.

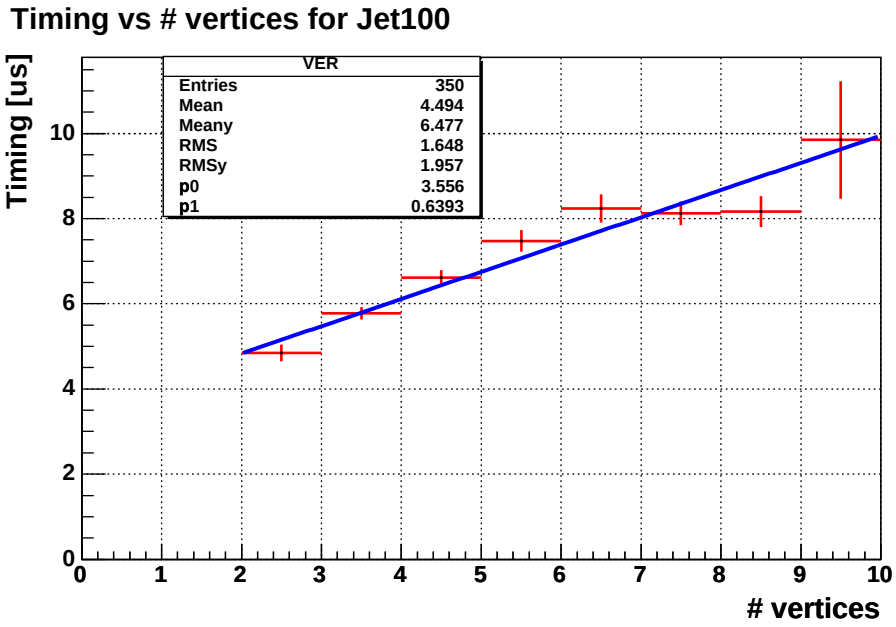

Figure 55: Clustering execution time as function of vertices.

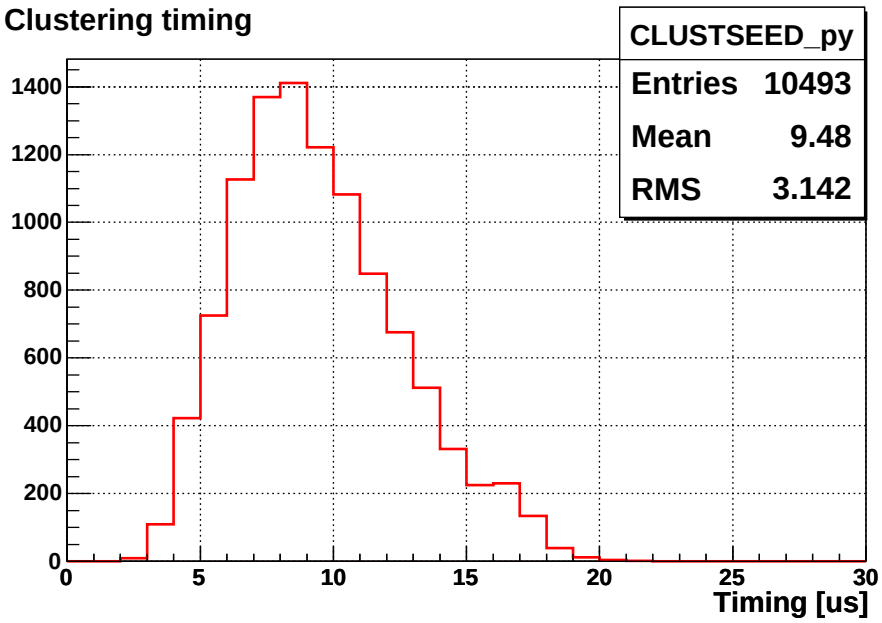

Figure 56: Code execution time for Jet100 sample combining with minimum bias sample.

As an extreme case (which is not realistic), we look at the execution time for the Jet100 sample when all towers are input into the calculation by using a seed and shoulder threshold of zero. Figure 57 shows the that the average execution time is $\sim 30\mu$s when a maximum of 20 clusters are reconstructed, and $\sim 42\mu$s, going as high as $\sim 50\mu$s when no limit is set on the number of clusters reconstructed. Nevertheless, work to further improve the execution time is ongoing.

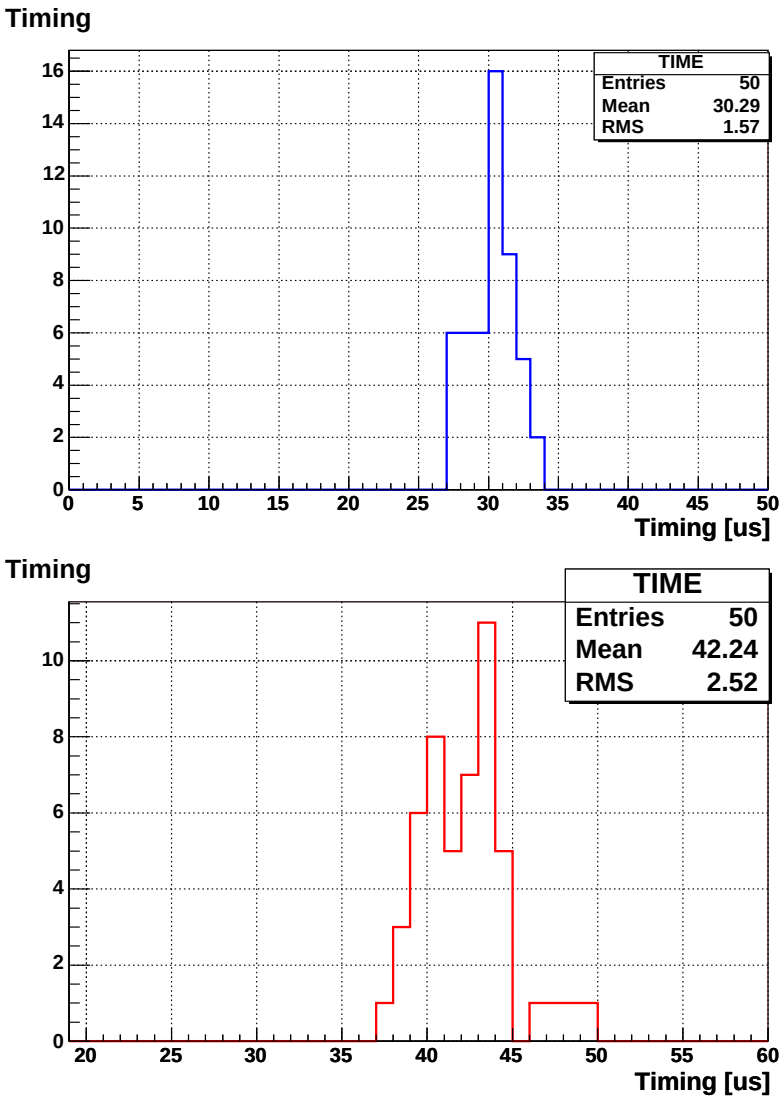

Figure 57: Code execution time for the Jet100 sample when a seed and shoulder threshold of zero is used for the clustering and (*top*) a maximum of 20 clusters are reconstructed and (*bottom*) no limit is set on the number of clusters.

Figure 58 shows the execution time for the $\not\!\!E_T$ calculation as a function of the number of towers which come into the calculation. This figure indicates that the $\not\!\!E_T$ calculation does not dramatically affect the timing of the algorithm, even in the worst case of all 576 input towers. In fact, in the worst case where all towers are needed, the timing is $\sim$2.3μs, which is a small fraction of the global timing. However, work to further improve the execution time is also ongoing for the $\not\!\!E_T$ calculation.

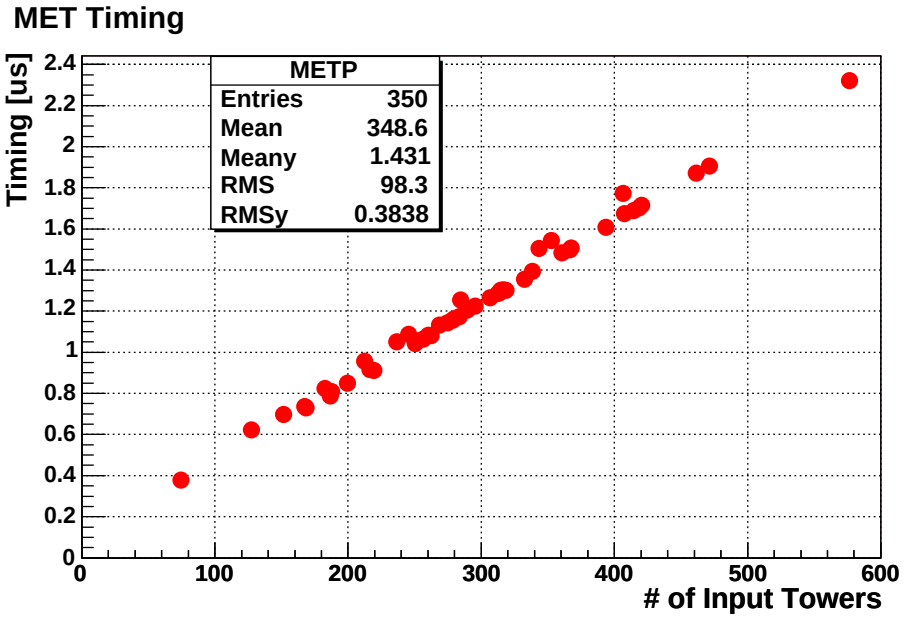

Figure 58: Time distribution for MET calculation

3.3 Data volume

Figure 59 shows the number of DCAS towers that pass various E_T thresholds in the STT5 sample. This impacts the clustering execution time, and gives an estimate of how much information will need to be sent to the CPU to run the L2Cone algorithm. Figure 60 shows the mean number of towers above threshold as a function of instantaneous luminosity.

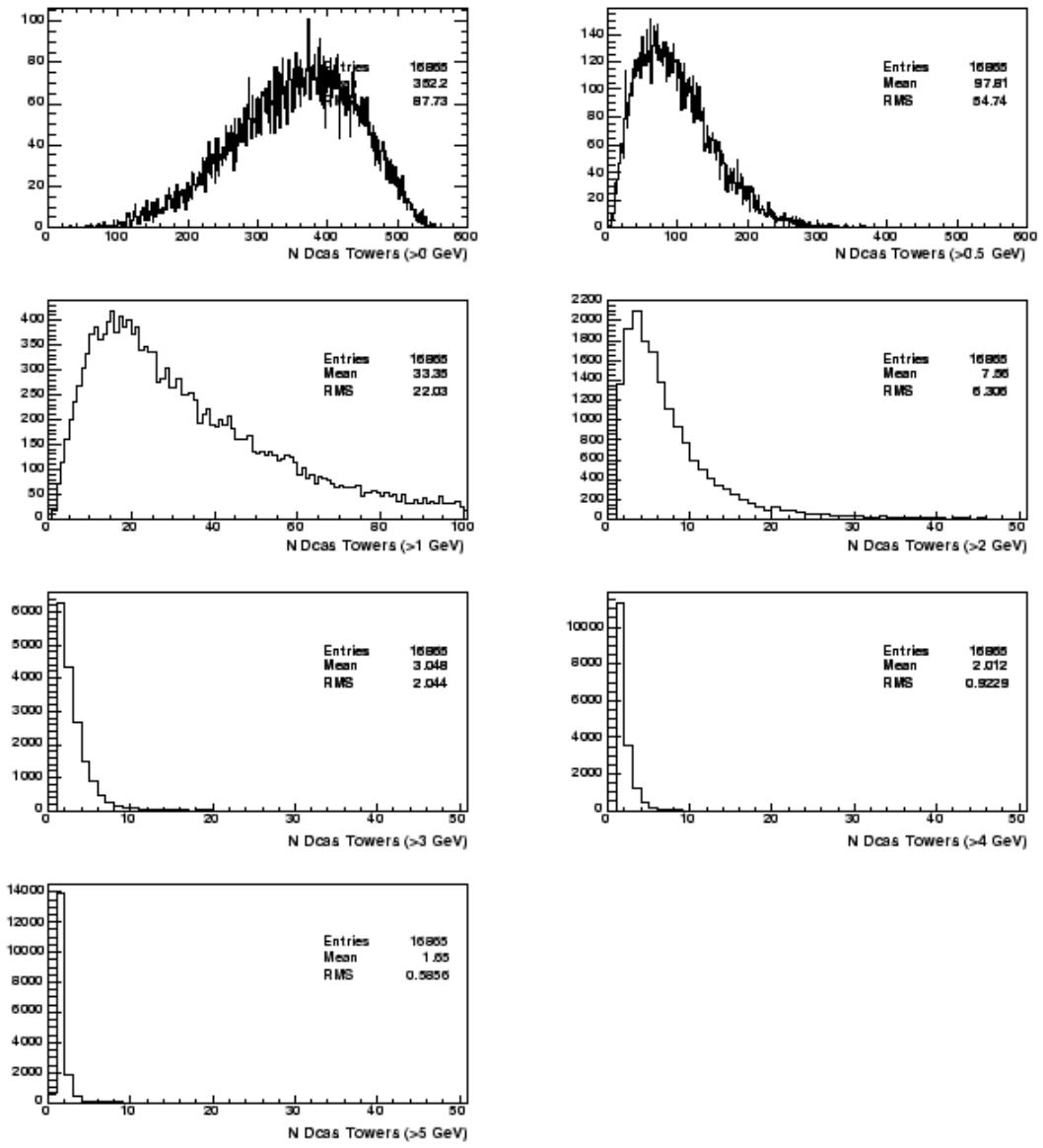

Figure 59: Number of DCAS towers that pass $E_T > 0$, 0.5, 1, 2, 3, 4, 5 GeV.

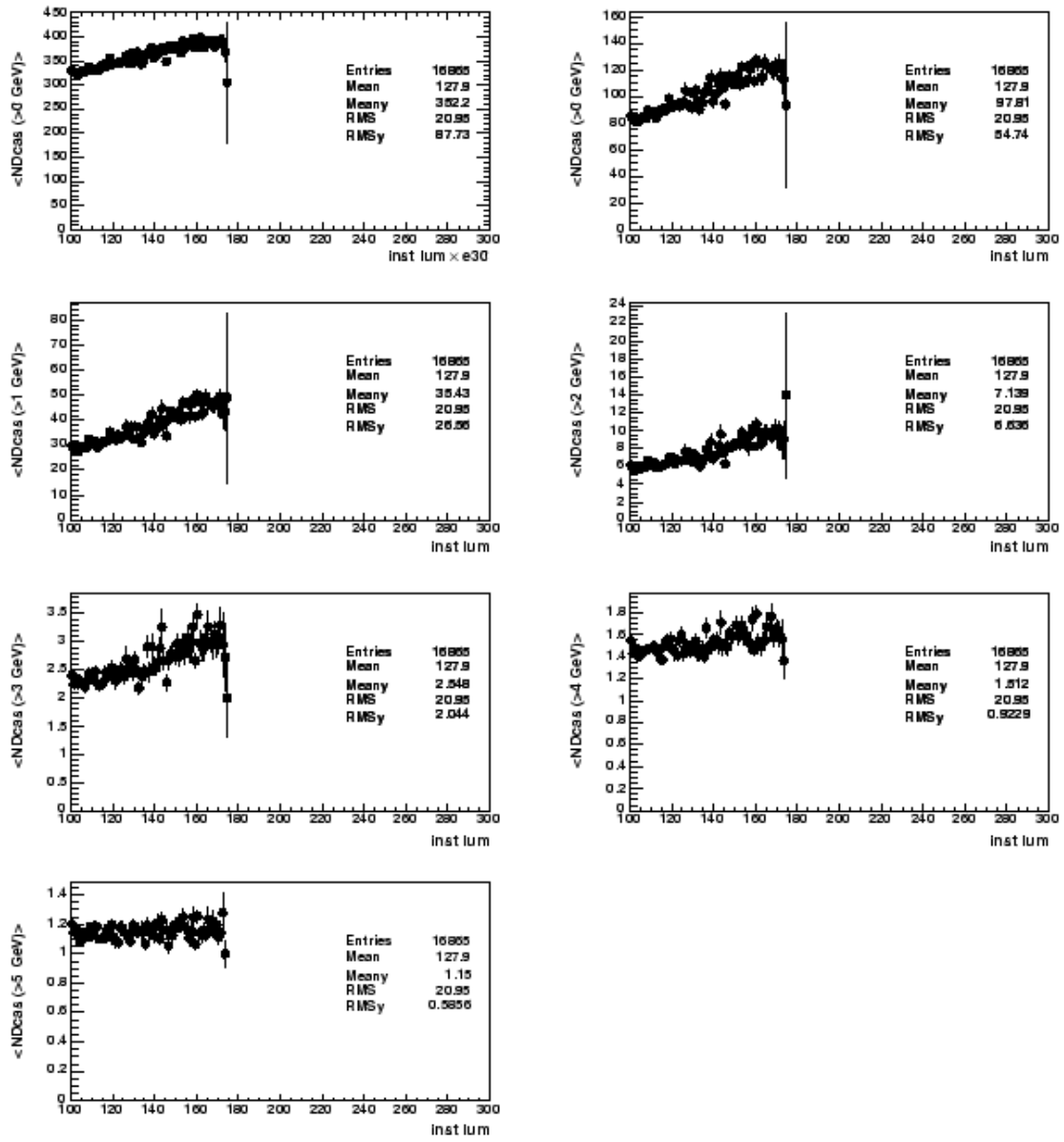

Figure 60: Mean number of DCAS towers that pass $E_T > 0$, 0.5, 1, 2, 3, 4, 5 GeV as a function of instantaneous luminosity.

4 Proposed L2CAL upgrade hardware configuration

At the hardware level, the basic idea of the L2CAL upgrade is to use Pulsar boards to receive the raw (full 10-bit resolution) trigger tower energy information from the DIRAC boards, merge and convert the data into SLINK format, then deliver the SLINK package to the L2 decision PC. This is very similar to what has been done to all the other L2 trigger data paths for the L2 decision Pulsar upgrade. In that sense, this can be viewed as a natural expansion of the L2 decision upgrade. In fact, since the clustering algorithm would now be done in software inside the L2 decision CPU, the proposed L2CAL system will be much simpler and much more uniform at the hardware (and firmware) level.

For the existing L2CAL system, since the actual clustering (also isolation) is done in hardware (designed in the mid 90's), the system is quite complicated. The entire system consists of 86 9U VME boards in 6 VME crates with a custom P3 backplane, including 72 DCAS, 6 LOCOS, 1 CLIQUE, 6 IsoPick and 1 Iso-Clique boards. The proposed L2CAL upgrade system will consist of 18 (new but identical to the present ones) Pulsar receiver boards, and 6 existing Pulsar SLINK merger boards. Since the Pulsar receiver only needs to receive the raw data and convert it into SLINK format, the firmware for the Pulsar receiver board will be simple. In order to receive the trigger tower energy LVDS signals from the DIRAC boards, a new Pulsar mezzanine card will need to be designed. One mezzanine card is able to receive 4 cables from DIRAC (corresponds to one DCAS input data), thus one Pulsar board can receive 16 cables or 4 DCAS input data.

Figure 61 shows the calorimeter related trigger subsystems for both Level 1 and Level 2, with the red part being the new L2CAL path. To minimize the impact on the running system, i.e. to be able to run in pure parasitic mode during commissioning, we will make a copy of the LVDS input signals (just as we did for all other L2 trigger paths for the L2 decision upgrade). In this case, we will use the LVDS "multi-drop" property, and make long cables in such a way (see Fig. 62) that each DIRAC output signal LVDS cable first has a "drop" at a Pulsar mezzanine card (without termination during commissioning), then goes to the existing DCAS input (which has 100 ohm termination). In other words, the signal splitting is simply being done with long cables having one additional connector (see Fig. 62).

In the current system, one DCAS board receives four input cables. In the new system, one Pulsar mezzanine card will receive the same amount of input data as one DCAS. Figure 63 shows the mezzanine card design. Note that the length of the mezzanine card will be doubled to allow easy access to all four LVDS cables. With four mezzanine cards per Pulsar board, 18 Pulsars (in two crates, see Fig 64) will be needed to receive all input data. The rest of the system consists of existing Pulsar SLINK mergers (see Fig. 65).

Note that the Pulsar based L2CAL will be very flexible, just like the rest of the Pulsar based L2 system. In fact, if really needed, it is even possible to implement the L1 MET trigger using the full 10-bit calorimeter energy information with Pulsar hardware.

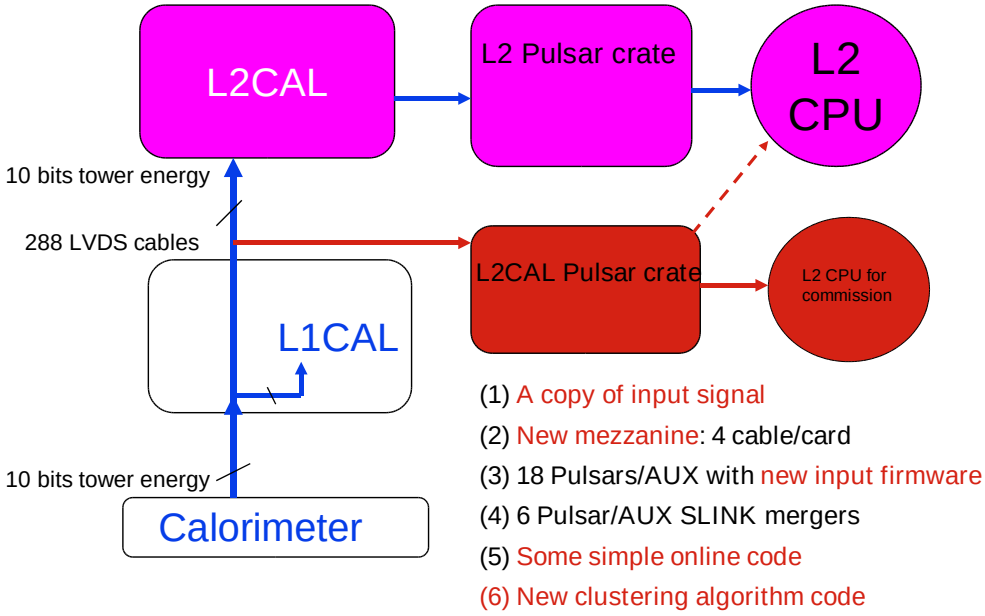

Figure 61: The red path represents the new hardware to be added to the calorimetric trigger system.

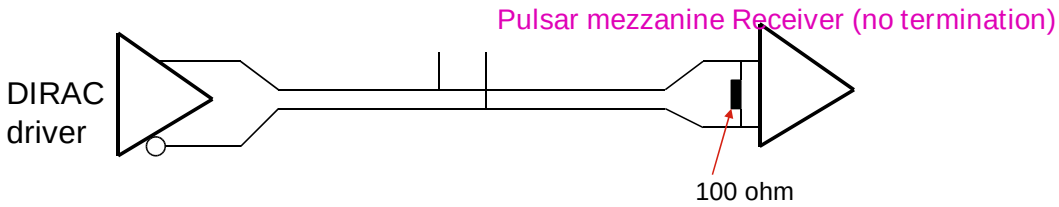

Figure 62: The bypass on the data path to operate the new and old systems together.

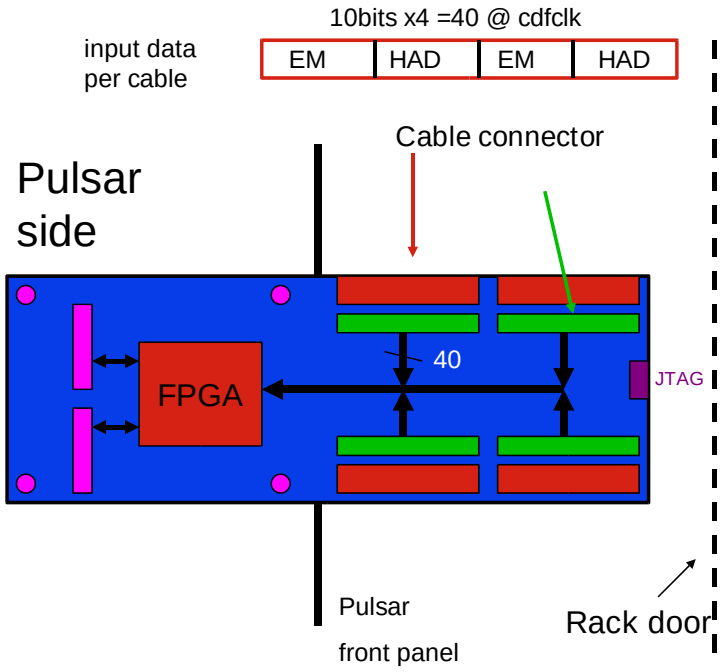

Figure 63: The mezzanine card that receives calorimetric data from DIRAC.

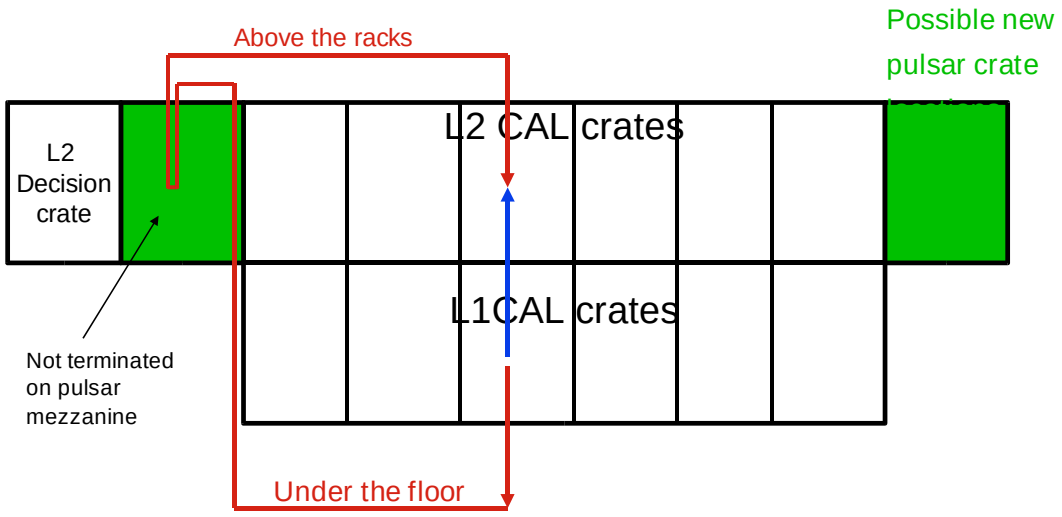

Figure 64: The new Pulsar crates (green) and the basic idea of new cabling (red).

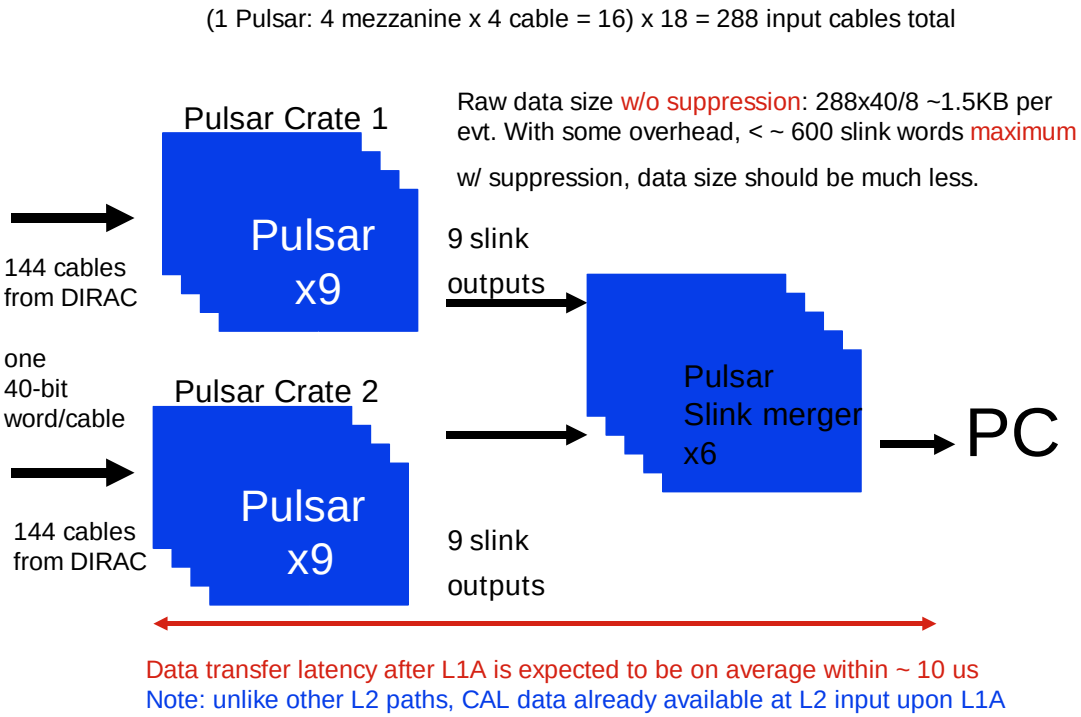

Figure 65: The 24 Pulsars to merge data from the DIRAC cards directly into the Level 2 decision PC. Data transfer from L1 accept to the L2 decision PC is expected to take on average less than $\sim 10\mu$s.

5 Implementation requirements

5.1 Upgrade and commissioning

As mentioned earlier, the proposed upgrade to L2CAL system is very similar to what has been done for all the other L2 trigger paths. The Pulsar and SVT groups have had extensive experience in the Pulsar hardware, mezzanine card design, firmware, SLINK merging, SLINK to PCI transfer, L2 algorithm code optimization, as well as online monitoring software, and parasitic commissioning strategies etc. Almost all of the tasks involved are familiar to us, and are listed below.

1. Input LVDS signal splitting: In order to be able to run in pure parasitic mode, one has to make a copy of the DCAS input signal from DIRAC (see earlier description).

2. Mezzanine card design: This mezzanine card will be very similar to all the other Pulsar mezzanine cards designed for other L2 trigger paths.

3. Pulsar firmware: Since all algorithm work can be done in L2 decision CPU, the Pulsar firmware should be simple as well. In fact, most of the firmware will be the same as the Pulsar firmware for the other L2 trigger paths, except for the input interface.

4. Readout software: The readout will be almost the same as existing Pulsar VME readout code, with some modifications for the formation of the final bank (to make it look exactly like the existing DCAS bank).

5. Online monitoring code: This will be relatively easy to implement in the existing PulsarMon package.

6. Clustering algorithm code inside CPU: The work already started a few months ago and is now in reasonably good shape. The code is also already optimized to a point where the performance is quite good. Still there is room for more improvements in the near future.

7. Final commissioning: All tasks (1-6) can be done in parallel before final commissioning. The final commissioning will be done in pure parasitic mode first. We could run the full L2 algorithm (with the new L2 clustering) inside another L2 decision CPU. We expect most of the work (and time) will be spent here, but the general commissioning strategy (and techniques used) is exactly the same as what we did for the L2 Pulsar commissioning (vs. Alpha system).

5.2 Cost

The only new hardware is the mezzanine card, which needs to be designed. The estimated cost is about \$50K, including final production ($\sim$100 of them, 72 needed in the system). Depending on how many other new projects will use Pulsar hardware, we may need to order more Pulsar hardware. Details will be discussed at the review on July 27th, 2006.

5.3 Schedule

We expect the hardware, firmware and software, including system installation, can be done in ∼6 months. It may take another few months to fully make use of the new L2CAL trigger capabilities in the official trigger table.

5.4 People

Only people who will be spending more than 20% of their time on the project are shown here.

Engineers:

- Marco Piendibene (50%): Pisa , engineer (already Pulsar firmware expert)
- Lucas Rogondino (100%): Pisa, engineer student
- Mircea Bogdan or Fukun Tang (part time): UC engineer for mezzanine card design (Pulsar hardware engineer)
- Richard Northrop (part time): UC mechanical engineer on cabling
- Harold Sanders (part time): UC
- Devis Pantano (30%): Padova technician

Physicists: postdocs:

- Laura Sartori (100%): Pisa
- Gene Flanagan (100%): Purdue
- Giorgio Cortiana (100%): Padova
- New Padova postdoc (100%): available end of the year
- New U. Chicago postdoc (H. Frisch) (100%): available later this year

Ph.D students:

- Miguel Vidal (100%): Madrid, available Sept. 2006
- Michael Schmidt (30%): U. Chicago (Y.K. Kim), available Sept. 2006
- New student from Purdue

5.5 Impact on data-taking

The final commissioning will be done in pure parasitic mode first. Together with a copy of the existing L2 system, the full L2 algorithm (with the new L2 clustering) would be run inside another L2 decision CPU. This would minimize the impact on the running system. This is the same commissioning strategy/technique as was used for the L2 Pulsar commissioning. Nothing new or risky is involved.

5.6 Impact on physics analysis

The level of effort required to extract physics using the upgraded L2 clustering would be minimal for the use of existing triggers. More effort will be put into improving triggers based on new possibilities made available by the upgrade. Much might be gained, for example, in Higgs sensitivity, by taking advantage of this upgrade.

Studies of trigger efficiencies for triggers involving jets or MET would have to be repeated; this would have to be done anyway for the higher luminosity data. Efficiencies are expected to be improved and more stable against luminosity.

Studies of b-tagging might also have to be repeated, if we make use of the possibility to better match jets and SVT tracks at the trigger level. Again, this would have to be done anyway for the higher luminosity data.

Understanding differences in datasets due to the change of clustering algorithms could be addressed with backup triggers and emulation of the old or new clustering algorithms as is being done in the studies shown in this proposal.

Options for new triggers based on the new information made available at Level 2 by this upgrade will have to be studied by the physics groups (in which many of the proponents of this proposal are also involved). It is likely that much can be gained. Purity of triggers would be improved, reducing L2 bandwidth or possibly allowing trigger cuts which were imposed to keep the rates down at high luminosity to be relaxed. Trigger turn-on efficiencies will be improved, possibly allowing thresholds to be decreased. Correlations between calorimeter quantities, e.g., $\Delta\phi$ between jets and MET, might be useful to reduce physics backgrounds at the trigger level. Triggers requiring b-jets could benefit from matching jets to SVT tracks at the trigger level, taking advantage of the much improved L2 position of the jet.

6 Conclusions

The proposed upgrade to the Level-2 calorimeter trigger system will provide a large overall reduction of the L2 trigger rate at high luminosity by significantly improving the purity of calorimeter-based triggers. Extensive studies have shown that the new system will be fast enough, yet there is still room for improvement. Without this upgrade, the CDF Run IIb physics program will be seriously jeopardized at high Tevatron luminosity. The full calorimeter trigger tower information is made available directly to the L2 decision CPU, which provides flexibility, allowing sophisticated algorithms to be implemented. The new L2 jet clustering will provide L2 jets which are nearly equivalent to offline jets in terms of E_T, centroid, and efficiency, and MET can be calculated more precisely at Level 2. Many important high-p_T triggers, notably the Higgs/SUSY trigger requiring MET and two jets, will benefit from this upgrade both in purity and efficiency in a significant way. The improved purity would allow the triggers to survive at the highest luminosities, while the improved efficiency could significantly push our Higgs sensitivity beyond the baseline. This is highly relevant given the recent attention being focused on the light Higgs.

Trigger	**Cross section (nb)**		
	100E30	**200E30**	**300E30**
Higgs high-p_T b-jet (loose)			
L2_BJET15_D120_DPS	160	DPS	
Higgs high-p_T b-jet			
L2_BJET15_D120_JET10_ETA1.8	56	316	866
$(W/Z \rightarrow \text{dijet}) + \gamma$			
L2_CEM12_ISO_&_SUMET20_&_TWO_JET3_ETA1.8	82	68	53
SUSY searches, Higgs			
L2_CJET10_JET10_L1_MET25_&_MET35_&_CJET_&_JET	136	867	2461
$\mu\tau$ for Higgs and exotic searches			
L2_CJET15_L1_BMU10_BSUR_TSUO	15	49	117
top multi-jet			
L2_FOUR_JET15_SUMET175	5	16	41
QCD jet studies, jet energy/resolution, b-tag studies, backup			
L2_CJET15_PS24	18	37	73
L2_JET15_PS25	39	94	202
L2_JET40	28	147	411
L2_JET60	21	53	120
new physics searches			
L2_JET90	25	42	79
high-p_T b-jet (loose)			
L2_TWO_JET15_ETA1.5_&_TWO_TRK2_D100_DPS	440	DPS	
$\not\!\!E_T + b$-jet ($ZH \rightarrow \nu\nu b\bar{b}$, SUSY, leptoquarks)			
L2_TWO_TRK2_D100_&_BJET15_&_MET15_DPS	240	DPS	
Higgs Multi-jet			
L2_TWO_TRK2_D120_&_THREE_JET10_SUMET90_DPS	90	DPS	
b-jet energy scale and resolution for top mass, Higgs			
L2_Z_BB_BJET_OS	24	lum enable 150	
L2_Z_BB_BJET_SS	18	lum enable 150	

Table 1: Triggers involving jets at Level 2 in the current trigger table PHYSICS_4_00 [3,798,638] and cross sections based on XMon predictions (which tend to underestimate cross sections at the highest luminosities).

References

[1] R. Blair *et al.* (CDF II collaboration), "The CDF Run II Detector Technical Design Report", 1996, FERMILAB-Pub-96/390-E.

[2] H.J. Frisch *et al.*, "Trigger tower organization and summing in η-ϕ space for Run II and beyond", CDF 2045.

[3] http://hep.uchicago.edu/∼thliu/projects/Pulsar

[4] K. Anikeev *et al.*, "CDF Level 2 Trigger Upgrade", IEEE Trans. on Nucl. Sci., Vol. 53, No 2, 2006 pp. 653 - 658.

[5] J. Adelman *et al.*, "First Steps in the Silicon Vertex Trigger upgrade at CDF", Nuclear Science Symposium Conference Record, 2005 IEEE Vol. 1, October 23 - 29, 2005, pp:603-607.